

Robust Differentiable Predictive Control with Safety Guarantees: A Predictive Safety Filter Approach

Wenceslao Shaw Cortez, Jan Drgona, Draguna Vrabić, Mahantesh Halappanavar

Abstract

In this paper, we propose a novel predictive safety filter that is robust to bounded perturbations and is combined with a learning-based control called differentiable predictive control (DPC). The proposed method provides rigorous guarantees of safety in the presence of bounded perturbations and implements DPC so long as the DPC control satisfies the system constraints. The approach also incorporates two forms of event-triggering to reduce online computation. The approach is comprised of a robust predictive safety filter that extends upon existing work to reject disturbances for discrete-time, time-varying nonlinear systems with time-varying constraints. The safety filter is based on novel concepts of robust, discrete-time barrier functions and can be used to filter any control law. Here we use the safety filter in conjunction with DPC as a promising policy optimization method. The approach is demonstrated on a single-integrator, two-tank system, and building example.

1 Introduction

Control barrier functions (CBFs) are a useful tool for ensuring constraint satisfaction of nonlinear, dynamical systems [1]. This method has received increasing attention in recent years due to its modularity and applicability to learning-based techniques that generally do not have guarantees of constraint satisfaction, i.e., safety. CBFs are also advantageous for being robust to unknown perturbations and provide asymptotic stability to the safe set. Robustness to perturbations allows for direct compensation of bounded disturbances to keep the system safe, while asymptotic stability to the safe set provides a recovery mechanism to return to the safe set.

One criticism of barrier function methods, however, is

Email addresses: w.shawcortez@pnnl.gov (Wenceslao Shaw Cortez), jan.drgona@pnnl.gov (Jan Drgona), draguna.vrabi@pnnl.gov (Draguna Vrabić), mahantesh.halappanavar@pnnl.gov (Mahantesh Halappanavar).

¹ The authors are with the Data Science and Machine Intelligence Department at the Pacific Northwest National Laboratory, Richland, WA, USA. This research was partially supported by the U.S. Department of Energy, through the Office of Advanced Scientific Computing Research’s “Data-Driven Decision Control for Complex Systems (DnC2S)” project, and through the Energy Efficiency and Renewable Energy, Building Technologies Office under the “Advancing Market-Ready Building Energy Management by Cost-Effective Differentiable Predictive Control” projects. PNNL is a multi-program national laboratory operated for the U.S. Department of Energy (DOE) by Battelle Memorial Institute under Contract No. DE-AC05-76RL0-1830.

the difficulty in constructing the functions themselves. [2] provides a way to construct barrier functions using maximal output admissible sets but is dependent on known stabilizing control law. Verification methods have been developed for uncertain system dynamics [3], but only probabilistic guarantees of safety are provided. Some synthesis methods are restricted to specific types of systems [4] or are dependent on sampling methods or sum-of-squares techniques, which do not scale well with system size [5]. Other approaches require expert-provided trajectories in order to learn the barrier function [6, 7]. Many of these approaches require significant offline data and computation, may be subject to conservatism, and are generally restricted to time-invariant systems. An alternative approach considered here is to use a prediction horizon to relax the conservatism of many of the existing methods.

Many existing barrier function methods claim superiority over model predictive control (MPC) due to the lower computational complexity required to implement barrier function methods. However, many such barrier function methods implement the safety-critical control as a nonlinear program, which is effectively a 1-step look-ahead MPC problem. The ability to predict system behavior can relax conservatism in the 1-step look-ahead approach. There exist methods that combine the finite horizon, MPC setup with control barrier functions [8–12]. In [8], a MPC-like optimization problem is constructed that acts as a barrier function for continuous-time, time-invariant, nonlinear systems. In [9], a discrete-time *predictive safety filter* is developed for discrete-time, time-invariant, nonlinear systems that is always guaranteed to be feasible and ensures

asymptotic stability to the safe set. In [10], safety and asymptotic stability are addressed by combining MPC with control barrier functions for discrete-time, nonlinear, time-invariant systems. In [11], barrier functions are used to ensure the safety of an MPC control law for a sampled-data, perturbed, nonlinear affine system. In [12], a disturbance observer is combined with an MPC-based barrier function control law to guarantee the safety of perturbed nonlinear, time-invariant, discrete-time systems with measurement noise. We note that many of the existing MPC-type methods that incorporate predictions with barrier functions for discrete-time systems lack robustness guarantees to handle perturbations and/or are restricted to time-invariant systems. Disturbance rejection is important for handling model mismatch, which is inevitable in practical applications. These restrictions exclude many real-world applications, such as buildings, wherein the dynamics change over time and are subject to time-varying constraints [13]. An alternative approach to address robustness is via a data-driven approach, typically restricted to special classes of systems (e.g., linear systems, time-invariant systems) or restricted to probabilistic guarantees. For an in-depth overview of the literature on data-driven safety filters, we refer the reader to [14, 15].

Existing discrete-time barrier methods have been applied to bipedal robotics [16] and adaptive high-order systems [17], for example, but there is a limited range of methods for handling bounded perturbations. [18] presents a robust barrier function that uses GP estimate of disturbance, but no hard guarantees of safety are provided. [19] presents discrete-time barrier functions that are robust to stochastic perturbations. [20] use discrete-time barriers for multi-agent partially observable Markov decision processes for probabilistic safety guarantees. [21] uses MPC in combination with discrete-time barriers, but no formal guarantees of safety are provided. [22] combines discrete-time high-order barriers in an MPC framework. [10] combines nonlinear MPC with discrete-time barriers, focusing on enhancing feasibility. [23] uses MPC with discrete-time barriers for obstacle avoidance. Apart from [18], [19] [9], and [12], none of the previous methodologies address robustness to perturbations. The methods from [18] [19] only address probabilistic safety, whereas the asymptotic stability results from [9] are effective for vanishing perturbations, but not for bounded, non-vanishing perturbations which are common in practice. In the continuous-time domain, there exist many solutions that are robust to bounded perturbations [24, 25], but this has been lacking in the discrete-time domain. Furthermore, all of the aforementioned approaches require constant online computation of optimization problems, which can be restrictive for computationally-limited edge devices.

Of the existing formulations, we focus to improve upon the discrete-time *predictive safety filter* from [9], which offers several advantages. The predictive safety filter pro-

vides a trade-off between conservatism and computational complexity in the sense that a conservative barrier function is used to construct the terminal set, but less conservative constraint conditions can be enforced *without* the construction of any additional barrier functions. Also, the predictive safety filter is always guaranteed to be feasible and ensures asymptotic stability to the safe set in the presence of unknown, vanishing perturbations.

In this work, we extend the predictive safety filter to address bounded perturbations as well as time-varying systems and constraints. Furthermore, we combine the safety filter to address performance and computation demand in a two-pronged approach. First, we use differentiable predictive control (DPC), which is an offline policy optimization algorithm based on direct policy gradients obtained by differentiating the parametric MPC problem [26]. The DPC method incorporates MPC objectives in the physics-informed loss function, in addition to constraint penalties to avoid violating system constraints. As a result, DPC is probabilistically optimal but not guaranteed to be safe in the presence of perturbations. However, the advantage of DPC lies in its systematic model-based approach to training neural control policies that allow for the integration of safety considerations such as Lyapunov functions or CBFs in the end-to-end learning pipeline [27, 28].

Second, we combine the safety filter with an event-triggered scheme. This event triggering only requires solving the safety filter optimization problem if the DPC control performs an unsafe action. By combining these methods together, we exploit the probabilistic, high-performing nature of the DPC controller with the event-triggering to reduce the overall online computation required to implement the proposed control. The resulting methodology is guaranteed to be safe and robust. Figure 1 illustrates the proposed method. The main contributions of this work are listed below:

- (1) Robust formulation of discrete-time barrier functions for 1-step ahead and N-step ahead safety filters in the presence of bounded perturbations.
- (2) Extension of the (robust) predictive safety filter results to time-varying systems and constraints.
- (3) Novel event-triggering methods for reducing online computations.
- (4) Guarantees of safety for DPC in the presence of perturbations.

The paper is outlined as follows. In Section 2, we introduce the robust barrier function formulations. In Section 3, we present the robust predictive safety filter to ensure safety in the presence of perturbations. In Section 4, we combine the predictive safety filter with DPC in an event-triggered control law to ensure safety while providing performance with lower online computational demand. In Section 5, we apply the proposed method to an integrator, a two-tank system, and a building system.

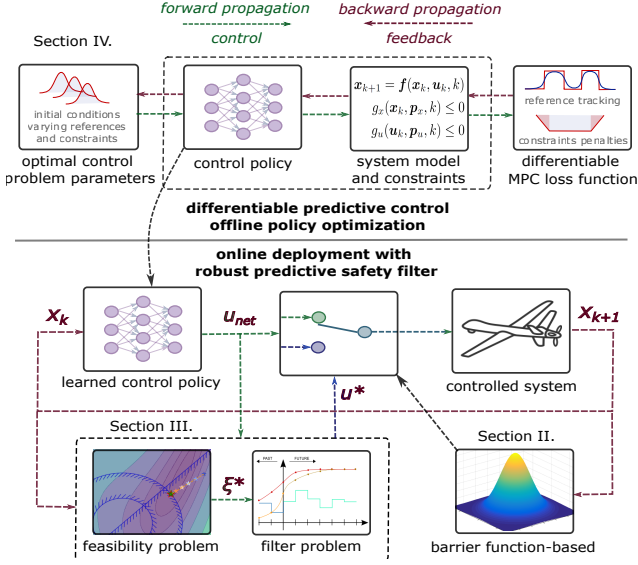


Fig. 1. Conceptual overview of the proposed event-triggered robust predictive safety filter combined with differentiable predictive control policy optimization.

Notation: Let \mathbb{N} be the set of natural numbers including 0. The interior and boundary of a set \mathcal{A} are denoted $\overset{\circ}{\mathcal{A}}$ and $\partial\mathcal{A}$, respectively. The notation \mathcal{L}_f^k is used to denote the Lipschitz constant of a Lipschitz function, $\mathbf{f}(\mathbf{x}, k)$, with respect to the second argument. Similarly, \mathcal{L}_f^x is used to denote the Lipschitz constant of \mathbf{f} with respect to the first argument. The notation \mathcal{L}_f will be used to denote a bound with respect to the function \mathbf{f} and will be explicitly defined in the text.

2 Robust Discrete-Time Barrier Functions

In this section, we present robustness guarantees and definitions for discrete-time barrier functions for 1-step and N-step look-ahead barrier functions.

Consider the following discrete-time dynamical system:

$$\mathbf{x}_{k+1} = \mathbf{f}(\mathbf{x}_k, \mathbf{u}_k, k) + \mathbf{d}(\mathbf{x}_k, \mathbf{u}_k, k), \quad \mathbf{x}_0 \in \mathbb{R}^n, k \in \mathbb{N} \quad (1)$$

where $\mathbf{f} : \mathbb{R}^n \times \mathbb{R}^m \times \mathbb{N} \rightarrow \mathbb{R}^n$ is a continuous function on its domain defining the known model, $\mathbf{u} \in \mathcal{U}$ is the control input for the compact set $\mathcal{U} \subset \mathbb{R}^m$, and $\mathbf{d} : \mathbb{R}^n \times \mathbb{N} \rightarrow \mathcal{D} \subset \mathbb{R}^n$ is a continuous function on its domain defining the disturbance for the compact set \mathcal{D} . For the compact set \mathcal{D} , let $\mathcal{L}_d \in \mathbb{R}_{\geq 0}$ be the bound of the disturbance defined as:

$$\mathcal{L}_d := \max_{\mathbf{x} \in \mathbb{R}^n, \mathbf{u} \in \mathcal{U}, k \in \mathbb{N}} \|\mathbf{d}(\mathbf{x}, \mathbf{u}, k)\| \quad (2)$$

s.t. $\mathbf{d}(\mathbf{x}, \mathbf{u}, k) \in \mathcal{D}$.

2.1 1-step Robust Discrete-Time Barrier Functions

Here, we extend the concept of a barrier function for discrete-time systems from [16, 17, 20] to address time-varying constraints and robustness to perturbations.

Consider a time-varying set defined by:

$$\mathcal{C}(k) = \{\mathbf{x} \in \mathbb{R}^n : h(\mathbf{x}, k) \geq 0\} \quad (3)$$

for the function $h : \mathbb{R}^n \times \mathbb{N} \rightarrow \mathbb{R}$, which is Lipschitz continuous on \mathbb{R}^n with Lipschitz constant \mathcal{L}_h^x . In this work, h will be used to indicate a discrete-time barrier function, whose formal definition will be given below.

To address robustness, we need to make sure that in the next time-instant, the system is able to offset the effect of the perturbation. To do so, we require that the control pushes the system sufficiently into the safe set to offset the potential worst-case effect of the perturbation. This is mathematically written as follows:

$$\delta h(\mathbf{x}, \mathbf{u}, k) := h(\mathbf{f}(\mathbf{x}, \mathbf{u}, k), k+1) - \mathcal{L}_h^x \mathcal{L}_d \geq 0 \quad (4)$$

We define the set of admissible control inputs for which (4) holds if $\mathbf{x}_k \in \mathcal{C}(k)$:

$$\mathcal{K}(\mathbf{x}, k) := \{\mathbf{u} \in \mathcal{U} : \delta h(\mathbf{x}, \mathbf{u}, k) \geq 0, \text{ if } \mathbf{x} \in \mathcal{C}(k)\} \quad (5)$$

We note that for notation purposes if $h(\mathbf{x}, k)$ is time-invariant, i.e., $h(\mathbf{x}, k) = h(\mathbf{x})$, then we will drop the dependency on k in related terms, e.g., \mathcal{C} , $\delta h(\mathbf{x}, \mathbf{u})$, and $\mathcal{K}(\mathbf{x})$.

Definition 1 Consider the system (1) and the function $h : \mathbb{R}^n \times \mathbb{N} \rightarrow \mathbb{R}$ with sets $\mathcal{C}(k)$ and $\mathcal{K}(\mathbf{x}, k)$ defined by (3) and (5) respectively, for which h is Lipschitz continuous on \mathbb{R}^n with Lipschitz constant \mathcal{L}_h^x . We say h is a robust, discrete-time barrier function, if $\mathcal{K}(\mathbf{x}, k) \neq \emptyset, \forall \mathbf{x} \in \mathcal{C}(k), \forall k \in \mathbb{N}$.

In the next theorem, we use the robust, discrete-time barrier functions to guarantee forward invariance of the safe set.

Theorem 2 Suppose h is a robust, discrete-time barrier function for (1). If $\mathbf{x}_{k_0} \in \mathcal{C}(k_0)$ for some $k_0 \in \mathbb{N}$ and $\mathbf{u}_k \in \mathcal{K}(\mathbf{x}_k, k)$ is implemented in closed-loop with (1), then $\mathbf{x}_k \in \mathcal{C}(k)$ for all $k \geq k_0, k \in \mathbb{N}$.

PROOF. By Lipschitz continuity of h , the following

holds for any $k \in \mathbb{N}$:

$$\begin{aligned} & |h(\mathbf{f}(\mathbf{x}, \mathbf{u}_k, k) + \mathbf{d}(\mathbf{x}, \mathbf{u}_k, k), k+1) - h(\mathbf{f}(\mathbf{x}, \mathbf{u}_k, k), k+1)| \\ & \leq \mathcal{L}_h^x \|\mathbf{f}(\mathbf{x}, \mathbf{u}_k, k) + \mathbf{d}(\mathbf{x}, \mathbf{u}_k, k) - \mathbf{f}(\mathbf{x}, \mathbf{u}_k, k)\| \\ & = \mathcal{L}_h^x \|\mathbf{d}(\mathbf{x}, \mathbf{u}_k, k)\| \\ & \leq \mathcal{L}_h^x \mathcal{L}_d \end{aligned}$$

It follows then that $h(\mathbf{f}(\mathbf{x}, \mathbf{u}_k, k), k+1) - \mathcal{L}_h^x \mathcal{L}_d \leq h(\mathbf{f}(\mathbf{x}, \mathbf{u}_k, k) + \mathbf{d}(\mathbf{x}, \mathbf{u}_k, k), k+1) = h(\mathbf{x}_{k+1}, k+1)$. Thus from (4), $h(\mathbf{x}_{k_0+1}, k_0+1) \geq h(\mathbf{f}(\mathbf{x}_{k_0}, \mathbf{u}_{k_0}, k_0), k_0+1) - \mathcal{L}_h^x \mathcal{L}_d \geq 0$. Thus $\mathbf{x}_{k_0+1} \in \mathcal{C}(k_0+1)$. Now it is clear that since $\mathbf{x}_{k_0} \in \mathcal{C}(k_0)$, then by induction $\mathbf{x}_k \in \mathcal{C}(k)$ for all $k \geq k_0$.

In special cases, we can ensure forward invariance without checking \mathcal{K} over all $\mathcal{C}(k)$. This can be thought of as a ‘one-step event-triggered’ condition defined as follows.

Let $\mathcal{A}(k) \subset \mathbb{R}^n$ be a set encompassing the boundary of $\mathcal{C}(k)$, defined by $\partial\mathcal{C}(k) = \{\mathbf{x} \in \mathbb{R}^n : h(\mathbf{x}, k) = 0\}$, which is defined by:

$$\mathcal{A}(k) = \{\mathbf{x} \in \mathbb{R}^n : h(\mathbf{x}, k) \in [0, a]\} \quad (6)$$

for some $a \in \mathbb{R}_{>0}$. The set $\mathcal{A}(k)$ defines the region around the controlled safe set boundary, which is the only region where we care about *enforcing* the safe set condition, i.e., $h \geq 0$. In this respect, we define the set of admissible control inputs for which $h \geq 0$ holds if $\mathbf{x} \in \mathcal{A}(k)$:

$$\mathcal{K}(\mathbf{x}, k) := \{\mathbf{u} \in \mathcal{U} : \delta h(\mathbf{x}, \mathbf{u}, k) \geq 0, \text{ if } \mathbf{x} \in \mathcal{A}(k)\} \quad (7)$$

We note that in this case, for any k and $\mathbf{x} \in \mathcal{C}(k) \setminus \mathcal{A}(k)$, then $\mathcal{K}(\mathbf{x}, k) = \mathcal{U}$ and so we need only check $\mathcal{A}(k)$ to determine if h satisfies the conditions of Definition 1.

Theorem 3 *Suppose the conditions of Theorem 2 hold with $\mathcal{K}(\mathbf{x}, k)$ defined by (7), $\mathcal{A}(k)$ defined by (6), and h is Lipschitz continuous on \mathbb{N} with Lipschitz constant $\mathcal{L}_h^k \in \mathbb{R}_{\geq 0}$. Further suppose there exists $\mathcal{L}_f \in \mathbb{R}_{>0}$ such that the following holds for all $\mathbf{x} \in \mathbb{R}^n$, $\mathbf{u} \in \mathcal{U}$, $k \in \mathbb{N}$:*

$$\|\mathbf{f}(\mathbf{x}, \mathbf{u}, k) - \mathbf{x}\| \leq \mathcal{L}_f, \quad (8)$$

for which $a \geq \mathcal{L}_h^x(\mathcal{L}_f + \mathcal{L}_d) + \mathcal{L}_h^k$, and the resulting $\mathcal{A}(k) \neq \emptyset \forall k \in \mathbb{N}$. If $\mathbf{x}_{k_0} \in \mathcal{C}(k_0)$ for some $k_0 \in \mathbb{N}$, and $\mathbf{u}_k \in \mathcal{K}(\mathbf{x}_k, k)$ is implemented in closed-loop with (1), then $\mathbf{x}_k \in \mathcal{C}(k)$ for all $k \geq k_0$, $k \in \mathbb{N}$.

PROOF. Since the conditions of Theorem 2 hold on $\mathcal{A}(k) \subset \mathcal{C}(k)$, we need only consider the case when $\mathbf{x}_k \in \mathcal{C}(k) \setminus \mathcal{A}(k)$ (i.e. $h(\mathbf{x}_k, k) > a$). Let $\bar{\mathbf{f}}_k = \mathbf{f}(\mathbf{x}_k, \mathbf{u}_k, k) + \mathbf{d}(\mathbf{x}_k, \mathbf{u}_k, k)$ to simplify the notation, for which (8) and the triangle inequality yields:

$\|\bar{\mathbf{f}}_k - \mathbf{x}_k\| = \|\mathbf{f}(\mathbf{x}_k, \mathbf{u}_k, k) + \mathbf{d}(\mathbf{x}_k, \mathbf{u}_k, k) - \mathbf{x}_k\| \leq \|\mathbf{f}(\mathbf{x}_k, \mathbf{u}_k, k) - \mathbf{x}_k\| + \|\mathbf{d}(\mathbf{x}_k, \mathbf{u}_k, k)\| \leq \mathcal{L}_f + \mathcal{L}_d$. Using the following Lipschitz conditions: $|h(\mathbf{y}, k) - h(\mathbf{x}, k)| \leq \mathcal{L}_h^x \|\mathbf{y} - \mathbf{x}\|$, $|h(\mathbf{x}, k+1) - h(\mathbf{x}, k)| \leq \mathcal{L}_h^k$ and the triangle inequality, we arrive at the following inequality:

$$\begin{aligned} & |h(\bar{\mathbf{f}}_k, k+1) - h(\mathbf{x}_k, k)| \\ & = |h(\bar{\mathbf{f}}_k, k+1) - h(\bar{\mathbf{f}}_k, k) + h(\bar{\mathbf{f}}_k, k) - h(\mathbf{x}_k, k)| \\ & \leq |h(\bar{\mathbf{f}}_k, k) - h(\mathbf{x}_k, k)| + |h(\bar{\mathbf{f}}_k, k+1) - h(\bar{\mathbf{f}}_k, k)| \\ & \leq \mathcal{L}_h^x \|\bar{\mathbf{f}}_k - \mathbf{x}_k\| + \mathcal{L}_h^k \\ & \leq \mathcal{L}_h^x(\mathcal{L}_f + \mathcal{L}_d) + \mathcal{L}_h^k \\ & \leq a \end{aligned}$$

From this relation, it follows that $h(\mathbf{x}_{k_0+1}, k_0+1) \geq h(\mathbf{x}_{k_0}, k_0) - a > 0$. Since $\mathbf{x}_{k_0} \in \mathcal{C}(k_0)$, then by induction $\mathbf{x}_k \in \mathcal{C}(k)$ for all $k \geq k_0$.

Remark 4 *Theorem 3 provides a new condition of forward invariance for discrete-time systems that does not require checking the condition $\delta h(\mathbf{x}, \mathbf{u}, k) \geq 0$ for all states in \mathcal{C}_k . This extends the standard results of forward invariance from [29] (for which Theorem 3 provides a sufficient condition) by requiring stronger conditions of h and the system dynamics. Theorem 3 provides a similar notion of forward invariance used in continuous-time systems, for which one need-only check how the system behaves near the constraint boundary to ensure safety.*

2.2 Predictive Safety and N -step Robust Discrete-Time Barrier Functions

2.2.1 Predictive Safety

The previous results focus on one-step-ahead control strategies to ensure safety. In order to incorporate prediction, we extend the previous steps to ensure that future trajectories satisfy the safety conditions. To do so, we first define the prediction of a future state as:

$$\begin{aligned} \hat{\mathbf{x}}_{N|k} &= \hat{\mathbf{f}}(\mathbf{x}_k, \{\mathbf{u}_{l|k}\}_{l=0}^{N-1}, k) := \\ & \mathbf{f}(\dots \mathbf{f}(\mathbf{x}_k, \mathbf{u}_{0|k}, k), \dots, \mathbf{u}_{N-1|k}, k+N-1) \end{aligned} \quad (9)$$

where the notation $\{\mathbf{u}_{l|k}\}_{l=0}^N := \{\mathbf{u}_0, \mathbf{u}_1, \dots, \mathbf{u}_N\}$ is used to denote the set of inputs \mathbf{u}_{l+k} starting from time $l=0$ up to $l=N$. Similarly, the notation $\mathbf{x}_{N|k}$ is the state \mathbf{x}_{k+N} at time $k+N$ beginning from time k at which point $\hat{\mathbf{x}}_{0|k} = \mathbf{x}_k$.

Next, we consider a Lipschitz continuous function on \mathbb{R}^n , $b : \mathbb{R}^n \times \mathbb{N} \rightarrow \mathbb{R}$, that need *not* be a barrier function in any sense. This function b is used to define general system constraints that should be satisfied, whose related safe set is defined as follows:

$$\mathcal{X}(k) := \{\mathbf{x} \in \mathbb{R}^n : b(\mathbf{x}, k) \geq 0\} \quad (10)$$

Next, we extend the term δh to accommodate future predictions with respect to $\mathcal{X}(k)$. In order to do this, we require the assumption that \mathbf{f} is Lipschitz continuous with respect to \mathbb{R}^n :

Assumption 5 \mathbf{f} is Lipschitz continuous on \mathbb{R}^n with Lipschitz constant $\mathcal{L}_f^x \in \mathbb{R}_{\geq 0}$.

The prediction-based robustness condition extends the concept of (4) by anticipating the worst-case disturbance acting on the system in the future trajectories. This is defined as follows:

$$\begin{aligned} \delta \hat{b}_{N|k}(\mathbf{x}_k, \{\mathbf{u}_{l|k}\}_{l=0}^{N-1}, k) &:= b(\hat{\mathbf{f}}(\mathbf{x}_k, \{\mathbf{u}_{l|k}\}_{l=0}^{N-1}, k), k+N) \\ &\quad - \mathcal{L}_b^x \mathcal{L}_d \sum_{j=0}^{N-1} (\mathcal{L}_f^x)^j \geq 0 \end{aligned} \quad (11)$$

Finally, we define the following set of safety-admissible control actions as:

$$\begin{aligned} \hat{\mathcal{K}}_{N|k}(\mathbf{x}_k, k) &:= \{ \mathbf{u}_{i-1+k} \in \mathcal{U}, i \in [1, N] \subset \mathbb{N} : \\ &\quad \delta \hat{b}_{i|k}(\mathbf{x}_k, \{\mathbf{u}_{l|k}\}_{l=0}^{i-1}, k) \geq 0 \} \end{aligned} \quad (12)$$

In the following proposition, we show that control inputs that lie inside the predictive set of safety admissible actions from (12) ensure open-loop safety of the system over the finite horizon.

Proposition 6 Consider the system (1) for which Assumption 5 holds. Given a function $b : \mathbb{R}^n \times \mathbb{N} \rightarrow \mathbb{R}$, Lipschitz continuous on \mathbb{R}^n with Lipschitz constant $\mathcal{L}_b^x \in \mathbb{R}_{\geq 0}$, let $\hat{\mathcal{K}}_{N|k}$, $\delta \hat{b}_{N|k}$, and $\mathcal{X}(k)$ be defined by (12), (11), and (10) respectively. For a given $\mathbf{x}_{k_0} \in \mathcal{X}(k_0)$, and $k_0, N \in \mathbb{N}$, $N \geq 1$, if $\{\mathbf{u}_{l|k_0}\}_{l=0}^{N-1} \in \hat{\mathcal{K}}_{N|k_0}(\mathbf{x}_{k_0}, k_0)$ is applied to (1) in closed-loop from time k_0 to $N-1$, then $\mathbf{x}_k \in \mathcal{X}(k)$ for all $k \in [k_0, k_0 + N] \subset \mathbb{N}$.

PROOF. Let $i \in [1, N] \subset \mathbb{N}$. The proof follows by showing that the error between the unperturbed prediction $\hat{\mathbf{x}}_{i|k}$ (defined by (9)) and perturbed prediction $\mathbf{x}_{i|k}$ (defined by (1)) is appropriately bounded and that this bound is taken into account via $\delta \hat{b}_{i|k}$. Using the Lipschitz property of \mathbf{f} and the bound \mathcal{L}_d along with the triangle inequality yields:

$$\|\hat{\mathbf{x}}_{i|k_0} - \mathbf{x}_{i|k_0}\| = \|\mathbf{f}(\hat{\mathbf{x}}_{i-1|k_0}, \mathbf{u}_{i-1|k_0}, k_0 + i - 1) \quad (13)$$

$$- \mathbf{f}(\mathbf{x}_{i-1|k_0}, \mathbf{u}_{i-1|k_0}, k_0 + i - 1) \quad (14)$$

$$- \mathbf{d}(\mathbf{x}_{i-1|k_0}, \mathbf{u}_{i-1|k_0}, k_0 + i - 1)\| \quad (15)$$

$$\leq \mathcal{L}_d + \mathcal{L}_f^x \|\hat{\mathbf{x}}_{i-1|k_0} - \mathbf{x}_{i-1|k_0}\| \quad (16)$$

We repeatedly apply the above process until we reach $i = 1$. This can be written as follows for $F(y) = \mathcal{L}_d + \mathcal{L}_f^x y$ and $F_i(y) = \underbrace{F \circ F \circ \dots \circ F}_i(y)$:

$$\begin{aligned} \|\hat{\mathbf{x}}_{i|k} - \mathbf{x}_{i|k}\| &\leq \underbrace{F \circ F \circ \dots \circ F}_i(\|\hat{\mathbf{x}}_{0|k} - \mathbf{x}_{0|k}\|) \\ &= F_i(\|\hat{\mathbf{x}}_{0|k} - \mathbf{x}_{0|k}\|) \end{aligned}$$

Now since $\hat{\mathbf{x}}_{0|k_0} = \mathbf{x}_{0|k_0} = \mathbf{x}_{k_0}$, it is clear from the previous relation that $\|\hat{\mathbf{x}}_{i|k} - \mathbf{x}_{i|k}\| \leq F_i(0)$ for which by evaluation $F_i(0) = \mathcal{L}_d \sum_{j=0}^{i-1} (\mathcal{L}_f^x)^j$.

Due to Lipschitz continuity of b , the following holds: $|b(\hat{\mathbf{x}}_{i|k_0}, k_0 + i) - b(\mathbf{x}_{i|k_0}, k_0 + i)| \leq \mathcal{L}_b^x \|\hat{\mathbf{x}}_{i|k_0} - \mathbf{x}_{i|k_0}\|$. Thus from the previous relations we have: $|b(\hat{\mathbf{x}}_{i|k_0}, k_0 + i) - b(\mathbf{x}_{i|k_0}, k_0 + i)| \leq \mathcal{L}_b^x \mathcal{L}_d \sum_{j=0}^{i-1} (\mathcal{L}_f^x)^j$. This implies that:

$$b(\mathbf{x}_{i|k_0}, k_0 + i) \geq b(\hat{\mathbf{x}}_{i|k_0}, k_0 + i) - \mathcal{L}_b^x \mathcal{L}_d \sum_{j=0}^{i-1} (\mathcal{L}_f^x)^j \quad (17)$$

By assumption, since $\{\mathbf{u}_{l|k_0}\}_{l=0}^{N-1} \in \hat{\mathcal{K}}_{N|k}(\mathbf{x}_{k_0}, k_0)$, $\{\mathbf{u}_{l|k_0}\}_{l=0}^{i-1}$ satisfies: $\delta \hat{b}_{i|k_0}(\mathbf{x}_{k_0}, \{\mathbf{u}_{l|k_0}\}_{l=0}^{i-1}, k_0) \geq 0$ for which $b(\hat{\mathbf{x}}_{i|k_0}, k_0 + i) \geq \mathcal{L}_b^x \mathcal{L}_d \sum_{j=0}^{i-1} (\mathcal{L}_f^x)^j$ (see (9), (11)). Combined with (17) yields: $b(\mathbf{x}_{i|k_0}, k_0 + i) \geq b(\hat{\mathbf{x}}_{i|k_0}, k_0 + i) - \mathcal{L}_b^x \mathcal{L}_d \sum_{j=0}^{i-1} (\mathcal{L}_f^x)^j \geq 0$ such that $\mathbf{x}_{i|k_0} = \mathbf{x}_{k_0+i} \in \mathcal{X}(k_0 + i)$. Application of this for all $i \in [1, N] \subset \mathbb{N}$ with $k = k_0 + i$ completes the proof.

It is important to emphasize that Proposition 6 does *not* require that b is a barrier function in any sense. This result is a sufficient condition for ensuring that in the finite horizon, the safety conditions will be met.

2.2.2 N-step Robust Discrete-Time Barrier Functions

For ensuring safety in a *predictive* context, we require a new barrier function that addresses prediction in (4). This condition is written as follows:

$$\begin{aligned} \delta \bar{h}_N(\mathbf{x}_k, \mathbf{u}_k, k) &:= h(\mathbf{f}(\mathbf{x}_k, \mathbf{u}_k, k), k+1) - \mathcal{L}_h^x \mathcal{L}_d (\mathcal{L}_f^x)^{N-1} \\ &\geq 0 \end{aligned} \quad (18)$$

We define the *N-step robust, discrete-time barrier function* as follows:

$$\bar{\mathcal{K}}(\mathbf{x}, k) := \{ \mathbf{u} \in \mathcal{U} : \delta \bar{h}_N(\mathbf{x}, \mathbf{u}, k) \geq 0, \text{ if } \mathbf{x} \in \mathcal{C}(k) \} \quad (19)$$

Definition 7 Consider the system (1) for which Assumption 5 holds and the function $h : \mathbb{R}^n \times \mathbb{N} \rightarrow \mathbb{R}$ with sets $\mathcal{C}(k)$ and $\bar{\mathcal{K}}$ defined by (3) and (19) respectively, for which h is Lipschitz continuous on \mathbb{R}^n with Lipschitz constant \mathcal{L}_h^x . We say h is an N -step robust, discrete-time barrier function, if $\bar{\mathcal{K}}(\mathbf{x}, k) \neq \emptyset, \forall \mathbf{x} \in \mathcal{C}(k), \forall k \in \mathbb{N}$.

In the following section, the results from Proposition 6 will be used to ensure constraint satisfaction in the finite horizon and the N -step robust, discrete-time barrier function will be used to define the terminal set of the predictive safety filter.

3 Robust Predictive Safety Filter Control

In this section, we define a predictive safety filter control law that enforces the barrier function conditions presented in Section 2. We provide guarantees of safety and feasibility of the proposed control.

3.1 Predictive Control

Here we present the predictive safety filter [9] with robustness modifications from Section 2. Consider the functions $b, h : \mathbb{R}^n \times \mathbb{N} \rightarrow \mathbb{R}$, which are Lipschitz continuous² on \mathbb{R}^n . The function b defines any system constraint to be satisfied, and h is a N -step robust, discrete-time barrier function. Note that b does not need to be a barrier function. The robust predictive safety filter is defined by the following **feasibility problem** and **safety filter problem**, respectively:

$$\mathcal{P}_{\text{feas}}(\mathbf{x}_k, k) = \min_{\xi_{l|k}, \mathbf{u}_{l|k}} \alpha_f \xi_{N|k} + \sum_{l=0}^{N-1} |\xi_{l|k}| \quad (20a)$$

$$\text{s.t. } \forall l = 0, \dots, N-1 : \quad (20b)$$

$$\hat{\mathbf{x}}_{0|k} = \mathbf{x}_k, \quad (20c)$$

$$\hat{\mathbf{x}}_{l+1|k} = \mathbf{f}(\hat{\mathbf{x}}_{l|k}, \mathbf{u}_{l|k}, l+k) \quad (20d)$$

$$\mathbf{u}_{l|k} \in \mathcal{U}, \quad (20d)$$

$$b(\hat{\mathbf{x}}_{l|k}, l+k) \geq -\xi_{l|k} + l\Delta + \mathcal{L}_b^x \mathcal{L}_d \sum_{j=0}^{l-1} (\mathcal{L}_f^x)^j, \quad (20e)$$

$$h(\hat{\mathbf{x}}_{N|k}, k+N) \geq -\xi_{N|k} + \mathcal{L}_h^x \mathcal{L}_d (\mathcal{L}_f^x)^{N-1} \quad (20f)$$

$$\xi_{l|k} \geq 0, \xi_{N|k} \geq 0 \quad (20g)$$

² Lipschitz continuity on \mathbb{R}^n is used here to simplify the presentation. Lipschitz continuity can be defined locally, i.e., over a set $\mathcal{D} \supset \mathcal{C}(k), \forall k \in \mathbb{N}$

$$\mathcal{P}_{sf}(\mathbf{x}_k, k, \{\xi_{l|k}^*\}_{l=0}^N) = \operatorname{argmin}_{\mathbf{u}_{l|k}} \|\mathbf{u}_{nom}(\mathbf{x}_k, k) - \mathbf{u}_{0|k}\| \quad (21a)$$

$$\text{s.t. } \forall l = 0, \dots, N-1 :$$

$$\hat{\mathbf{x}}_{0|k} = \mathbf{x}_k, \quad (21b)$$

$$\hat{\mathbf{x}}_{l+1|k} = \mathbf{f}(\hat{\mathbf{x}}_{l|k}, \mathbf{u}_{l|k}, l+k) \quad (21c)$$

$$\mathbf{u}_{l|k} \in \mathcal{U}, \quad (21d)$$

$$b(\hat{\mathbf{x}}_{l|k}, l+k) \geq -\xi_{l|k}^* + l\Delta + \mathcal{L}_b^x \mathcal{L}_d \sum_{j=0}^{l-1} (\mathcal{L}_f^x)^j, \quad (21e)$$

$$h(\hat{\mathbf{x}}_{N|k}, k+N) \geq -\xi_{N|k}^* + \mathcal{L}_h^x \mathcal{L}_d (\mathcal{L}_f^x)^{N-1} \quad (21f)$$

$$\{\mathbf{u}_{l|k}^*\}_{l=0}^N = \mathcal{P}_{sf}(\mathbf{x}_k, k, \{\xi_{l|k}^*\}_{l=0}^N) \quad (22)$$

where the $\{\xi_{l|k}^*\}_{l=0}^N$ in (21) are the argmin solutions of (20), $\mathbf{u}_{nom} : \mathbb{R}^n \times \mathbb{N} \rightarrow \mathbb{R}^m$ is any given nominal control law, $\Delta \in \mathbb{R}_{\geq 0}$ is a small value to promote asymptotic stability to the safe set and $\alpha_f \in \mathbb{R}_{>0}$ is a weighting term that should be chosen sufficiently large (see [9] for further details). The predictive safety filter computation involves first solving (20) for the slack terms $\{\xi_{l|k}^*\}_{l=0}^N$, which ensure feasibility of (21). The solution of (21) is the predictive control law that enforces the safety condition, if $\{\xi_{l|k}^*\}_{l=0}^N = \mathbf{0}$, or else asymptotically approaches the safety set. The difference between the proposed robust predictive safety filter and that of [9] is the incorporation of robustness-related terms, i.e., $\mathcal{L}_b^x, \mathcal{L}_d, \mathcal{L}_h^x$, and \mathcal{L}_f^x . Without these robustness terms, the presence of any bounded disturbance can push the system outside of the safe set.

Remark 8 Note that the use of Δ in \mathcal{P}_{feas} and \mathcal{P}_{sf} is motivated by the asymptotic stability results of [9]. However, in our formulation Δ can be set to zero to only focus on forward invariance of the safe set. In future work, we aim to extend the asymptotic stability results of [9] to the time-varying system addressed here.

The terms b and h are two different constraints to be implemented. The h function acts as a terminal constraint that must be an N -step robust, discrete-time barrier function for robustness guarantees to hold, whereas b is any constraint function to be satisfied at all times. From a practical perspective, the h function must be constructed to satisfy the conditions of Definition 7, which will most likely result in a conservative terminal set. Thus for more aggressive, but safe performance, a designer would construct h conservatively, but then enlarge the prediction horizon, N . The constraints defined by b can then be satisfied without checking that b itself is a robust, discrete-time barrier function. The trade-off

is that as N increases, more computation is required to check that safety is guaranteed, while the system state is able to deviate further from the conservative bound defined by h . For a time-invariant h , the linearization approach from [9] can be used to construct h to satisfy Definition 7.

The predictive safety control can be implemented in a 1-step look-ahead fashion, typical of many existing barrier function methods. In this case, the proposed control can be simplified into the following optimization problems:

$$\begin{aligned} \mathcal{P}_{\text{feas}}(\mathbf{x}_k, k) = & \\ \min_{\xi_k, \mathbf{u}_k} & \alpha_f \xi_k & (23a) \\ \text{s.t.} & & \\ \hat{\mathbf{x}}_{0|k} = & \mathbf{x}_k, & (23b) \\ \hat{\mathbf{x}}_{1|k} = & \mathbf{f}(\hat{\mathbf{x}}_{0|k}, \mathbf{u}_k, k) & (23c) \\ \mathbf{u}_k \in & \mathcal{U}, & (23d) \\ h(\hat{\mathbf{x}}_{1|k}, k+1) \geq & -\xi_k + \mathcal{L}_h^x \mathcal{L}_d & (23e) \\ \xi_k \geq & 0 & (23f) \end{aligned}$$

$$\begin{aligned} \mathcal{P}_{\text{sf}}(\mathbf{x}_k, k, \xi_k^*) = & \\ \operatorname{argmin}_{\mathbf{u}_k} & \|\mathbf{u}_{\text{nom}}(\mathbf{x}_k, k) - \mathbf{u}_k\| & (24a) \\ \text{s.t.} & & (24b) \\ \hat{\mathbf{x}}_{0|k} = & \mathbf{x}_k, & (24c) \\ \hat{\mathbf{x}}_{1|k} = & \mathbf{f}(\hat{\mathbf{x}}_{0|k}, \mathbf{u}_k, k) & (24d) \\ \mathbf{u}_k \in & \mathcal{U}, & (24e) \\ h(\hat{\mathbf{x}}_{1|k}, k+1) \geq & -\xi_k^* + \mathcal{L}_h^x \mathcal{L}_d & (24f) \end{aligned}$$

3.2 Analysis

The following assumption is made regarding the terminal constraint function h :

Assumption 9 *The function $h : \mathbb{R}^n \times \mathbb{N} \rightarrow \mathbb{R}$ with corresponding sets $\mathcal{C}(k)$ and $\bar{\mathcal{K}}$ defined by (3) and (19), respectively, is an N -step robust, discrete-time barrier function. Furthermore h is Lipschitz continuous with respect to \mathbb{R}^n .*

In the following theorem, we show that the proposed control is always feasible and ensures the states remain inside of the safe set $\mathcal{X}(k)$ for all time in the presence of disturbances. To do so, we first define the predictive control barrier function similar to [9]:

$$h_{pb}(\mathbf{x}_k, k) := -\mathcal{P}(\mathbf{x}_k, k) \quad (25)$$

We define the safe set for the predictive barrier function as:

$$\mathcal{C}_{pb}(k) := \{\mathbf{x} \in \mathbb{R}^n : h_{pb}(\mathbf{x}, k) \geq 0\} \quad (26)$$

Let the robust safety set and robust terminal safe set be respectively defined by:

$$\begin{aligned} \mathcal{X}^l(\xi, k) = \{\mathbf{x} \in \mathbb{R}^n : b(\mathbf{x}, k) \geq -\xi + l\Delta + \mathcal{L}_b^x \mathcal{L}_d \sum_{j=0}^{l-1} (\mathcal{L}_f^x)^j\}, \\ \forall l \in \{0, \dots, N\} \quad (27) \end{aligned}$$

$$\mathcal{X}_f^N(\xi, k) = \{\mathbf{x} \in \mathbb{R}^n : h(\mathbf{x}, k) \geq -\xi + \mathcal{L}_h^x \mathcal{L}_d (\mathcal{L}_f^x)^{N-1}\} \quad (28)$$

The following assumption is required to ensure the robust safety sets are non-empty and that if the final state in the horizon lies in terminal robust safety set, then it also lies in the robust safety set, i.e., $\mathcal{X}_f^N(0, k+N) \subset \mathcal{X}^N(0, k+N)$, $\forall k \in \mathbb{N}$.

Assumption 10 *The following conditions hold:*

- (1) $\mathcal{X}^l(0, k+l) \neq \emptyset$, $\forall l \in \{0, \dots, N\}$, $\forall k \in \mathbb{N}$
- (2) $\mathcal{X}_f^N(0, k) \neq \emptyset$, $\forall k \in \mathbb{N}$
- (3) $\mathcal{X}_f^N(0, k+N) \subset \mathcal{X}^N(0, k+N)$, $\forall k \in \mathbb{N}$.

The following theorem presents one of the main results and states that the proposed robust safety filter ensures the states remain inside of the safe region $\mathcal{X}(k)$ and feasibility of the proposed control for all time. The main differences between this result and that of [9] is that here we address robustness to perturbations and extend the approach to time-varying systems with time-varying constraints. The proof follows by showing that if the slack terms from $\mathcal{P}_{\text{feas}}$ are zero, i.e., $\mathbf{x}_k \in \mathcal{C}_{pb}(k)$, then there always exists a control that can keep the system safe and return to the terminal safe set. This is similar to the concept of recursive feasibility in conventional MPC methods. The key in this proof is in handling the affect of the disturbances in all future predictions of the system by exploiting Proposition 6 and Definition 7.

Theorem 11 *Consider the system (1) satisfying Assumption 5. Given a function $b : \mathbb{R}^n \times \mathbb{N} \rightarrow \mathbb{R}$, which is Lipschitz continuous on \mathbb{R}^n with respective Lipschitz constant $\mathcal{L}_b^x \in \mathbb{R}_{\geq 0}$, let $\hat{\mathcal{K}}$, $\delta \hat{b}_{N|k}$, and $\mathcal{X}(k)$ be defined by (12), (11), and (10), respectively. For a given $h : \mathbb{R}^n \times \mathbb{N} \rightarrow \mathbb{R}$, suppose Assumptions 9 and 10 hold. For (1) in closed-loop with (20), (21), (22), let h_{pb} and $\mathcal{C}_{pb}(k)$ be defined by (25) and (26). The following hold:*

- (1) *The control defined by (20), (21), (22) is always feasible.*
- (2) *$\mathcal{C}_{pb}(k) \subset \mathcal{X}(k)$, $\forall k \in \mathbb{N}$*
- (3) *If, for any given $k_0 \in \mathbb{N}$, $\mathbf{x}_{k_0} \in \mathcal{C}_{pb}(k_0)$, then $\mathbf{x}_k \in \mathcal{X}(k)$ and $\mathbf{x}_k \in \mathcal{C}_{pb}(k)$ for all $k \geq k_0$, $k \in \mathbb{N}$.*

PROOF. 1) (This part is modified from the proof of Lemma C.1 of [9]) For feasibility, we first note that b , h , are well-defined on $\mathbb{R}^n \times \mathbb{N}$ and \mathbf{f} and \mathbf{d} are well-defined on $\mathbb{R}^n \times \mathbb{R}^m \times \mathbb{N}$. Furthermore, $\mathcal{P}_{\text{feas}}$ can be written as follows:

$$\begin{aligned} \mathcal{P}_{\text{feas}}(\mathbf{x}, k) = & \inf_{\mathbf{u}_i \in \mathcal{U}} \alpha_f \max(0, -h(\mathbf{f}(\dots \mathbf{f}(\mathbf{f}(\mathbf{x}, \mathbf{u}_0, k), \mathbf{u}_1, k+1), \dots, \\ & k+N-1), k+N) - \mathcal{L}_h^x \mathcal{L}_d (\mathcal{L}_f^x)^{N-1}) + \sum_{l=0}^{N-1} |\max(0, \\ & -b(\mathbf{f}(\dots \mathbf{f}(\mathbf{f}(\mathbf{x}, \mathbf{u}_0, k), \mathbf{u}_1, k+1, \dots), k+l) - l\Delta \\ & - \mathcal{L}_b^x \mathcal{L}_d \sum_{j=0}^{l-1} (\mathcal{L}_f^x)^j)| \quad (29) \end{aligned}$$

Since \mathbf{f} is continuous on its domain, the cost function in 29 is continuous with respect to \mathbf{u}_i and k . Since \mathcal{U} is compact, application of the Weierstrass Extreme Value [30][Prop A.7], ensures there exists a minimum for all $\mathbf{x} \in \mathbb{R}^n$, $k \in \mathbb{N}$. Thus $\mathcal{P}_{\text{feas}}$ is always feasible. Since the solution of $\mathcal{P}_{\text{feas}}$ satisfies the constraints of \mathcal{P}_{sf} , \mathcal{P}_{sf} is also always feasible.

2) By definition of $\mathcal{C}_{pb}(k)$ and h_{pb} , for any k for which $\mathbf{x}_k \in \mathcal{C}_{pb}(k)$, $\{\xi_{l|k}^*\}_{l=0}^N = 0$, and so $\mathbf{x}_k \in \mathcal{X}^l(0, k+l) \subset \mathcal{X}(k)$ for all $l \in \{0, \dots, N\}$. Since $\mathbf{x}_k \in \mathcal{C}_{pb}(k) \implies \mathbf{x}_k \in \mathcal{X}(k)$, it follows that $\mathcal{C}_{pb}(k) \subset \mathcal{X}(k)$.

3) To show that $\mathcal{C}_{pb}(k)$ is forward invariant, we need to show that for any k and $\mathbf{x}_k \in \mathcal{C}_{pb}(k)$, $\mathbf{x}_{k+1} \in \mathcal{C}_{pb}(k+1)$. By definition of $\mathcal{C}_{pb}(k)$ and h_{pb} , for any k for which $\mathbf{x}_k \in \mathcal{C}_{pb}(k)$, $\{\xi_{l|k}^*\}_{l=0}^N = 0$. Thus we need to show that $\mathcal{P}_{\text{feas}}(\mathbf{x}_{k+1}, k+1) = 0$. From 2), if $\mathcal{C}_{pb}(k)$ is forward invariant, then \mathbf{x}_k will also remain in $\mathcal{X}(k)$, $\forall k \geq k_0$.

For any k for which $\mathbf{x}_k \in \mathcal{C}_{pb}(k)$, the constraints in $\mathcal{P}_{\text{feas}}$ and \mathcal{P}_{sf} satisfy: $b(\hat{\mathbf{x}}_{l|k}, l+k) \geq l\Delta + \mathcal{L}_b^x \mathcal{L}_d \sum_{j=0}^{l-1} (\mathcal{L}_f^x)^j \geq \mathcal{L}_b^x \mathcal{L}_d \sum_{j=0}^{l-1} (\mathcal{L}_f^x)^j$, $\forall l \in \{1, \dots, N-1\} \implies \delta \hat{b}_{j|k}(\mathbf{x}_k, \{\mathbf{u}_{l|k}\}_{l=0}^{j-1}, k) \geq 0$, $\forall j \in \{1, \dots, N-1\}$. Thus by construction, $\{\mathbf{u}_{l|k}^*\}_{l=0}^{N-1} \in \hat{\mathcal{K}}_{N-1|k}(\mathbf{x}_k, k)$.

Proposition 6 then ensures that the open-loop application of $\{\mathbf{u}_{l|k}^*\}_{l=0}^{N-1}$ to (1), i.e., such that $\mathbf{u}_k = \mathbf{u}_{0|k}^*$, $\mathbf{u}_{k+1} = \mathbf{u}_{1|k}^*$, \dots , $\mathbf{u}_{k+N-1} = \mathbf{u}_{N-1|k}^*$, ensures that $\mathbf{x}_\kappa \in \mathcal{X}(\kappa)$ for all $\kappa \in \{k+1, \dots, k+N-1\}$. We will denote the resulting state trajectory associated with $\{\mathbf{u}_{l|k}^*\}_{l=0}^{N-1}$ applied to the unperturbed system (20c) as $\{\hat{\mathbf{x}}_{l|k}\}_{l=0}^N$, i.e., this is the predicted system trajectory with the optimal control at time k .

In the closed-loop response, we know that from Proposition 6, $\mathbf{x}_{k+1} \in \mathcal{X}(k+1)$. In order to show that

$\mathcal{P}_{\text{feas}}(\mathbf{x}_{k+1}, k+1) = 0$, we need to show that there exists a feasible control action such that at $k+1$, $\{\xi_{l|k+1}^*\}_{l=0}^N = 0$ is a feasible solution to $\mathcal{P}_{\text{feas}}(\mathbf{x}_{k+1}, k+1)$. The feasible control action chosen is defined as follows:

$$\mathbf{u}_{l|k+1}^+ \in \begin{cases} \{\mathbf{u}_{l+1|k}^*\}, \forall l \in \{0, \dots, N-2\}, \\ \bar{\mathcal{K}}(\hat{\mathbf{x}}_{N-1|k+1}, k+N), \text{ for } l = N-1 \\ \quad \text{if } \hat{\mathbf{x}}_{N-1|k+1} \in \mathcal{C}(k+N), \\ \{\mathbf{0}\}, \text{ for } l = N-1 \text{ if } \hat{\mathbf{x}}_{N-1|k+1} \notin \mathcal{C}(k+N) \end{cases} \quad (30)$$

for which the chosen control action yields an unperturbed trajectory $\{\hat{\mathbf{x}}_{l|k+1}\}_{l=0}^{N-1}$, where $\hat{\mathbf{x}}_{l|k+1}$ is defined by (20c) starting at time $k+1$ with $\hat{\mathbf{x}}_{0|k+1} = \mathbf{x}_{k+1}$. Note that $\{\hat{\mathbf{x}}_{l|k+1}\}_{l=0}^{N-1}$ may not be equal to $\{\hat{\mathbf{x}}_{l|k}\}_{l=1}^N$ because $\hat{\mathbf{x}}_{0|k+1} = \mathbf{x}_{k+1}$, i.e., the initial condition in the prediction of the unperturbed state at time $k+1$ is the result of the *true* system dynamics.

The last step here is to show that the control action (30) yields $\hat{\mathbf{x}}_{l|k+1}$ that satisfy $b(\hat{\mathbf{x}}_{l|k+1}, k+l+1) \geq l\Delta + \mathcal{L}_b^x \mathcal{L}_d \sum_{j=0}^{l-1} (\mathcal{L}_f^x)^j$ for all $l \in \{0, \dots, N-1\}$ and $h(\hat{\mathbf{x}}_{N|k+1}, k+N+1) \geq \mathcal{L}_h^x \mathcal{L}_d (\mathcal{L}_f^x)^{N-1}$.

We first follow a similar approach to the proof of Proposition 6 and define the error between the unperturbed trajectory at k , $\hat{\mathbf{x}}_{i+1|k}$, and the resulting trajectory from $\mathbf{u}_{i|k+1}^+$, $\hat{\mathbf{x}}_{i|k+1}$, for all $i \in \{0, \dots, N-1\}$ using the Lipschitz property of \mathbf{f} . Consider the following relation for $i \in \{1, \dots, N-1\}$:

$$\begin{aligned} \|\hat{\mathbf{x}}_{i|k+1} - \hat{\mathbf{x}}_{i+1|k}\| &= \|\mathbf{f}(\hat{\mathbf{x}}_{i-1|k+1}, \mathbf{u}_{i-1|k+1}^+, k+i) \\ &\quad - \mathbf{f}(\hat{\mathbf{x}}_{i|k}, \mathbf{u}_{i-1|k+1}^+, k+i)\| \\ &\leq \mathcal{L}_f^x \|\hat{\mathbf{x}}_{i-1|k+1} - \hat{\mathbf{x}}_{i|k}\| \quad (31) \end{aligned}$$

For each $i \in \{1, \dots, N-1\}$ we can repeat the application of (31) until $i=1$, which yields:

$$\|\hat{\mathbf{x}}_{i|k+1} - \hat{\mathbf{x}}_{i+1|k}\| \leq (\mathcal{L}_f^x)^i \|\hat{\mathbf{x}}_{0|k+1} - \hat{\mathbf{x}}_{1|k}\|$$

Now recall that $\hat{\mathbf{x}}_{0|k+1} = \mathbf{x}_{k+1} = \mathbf{f}(\mathbf{x}_k, \mathbf{u}_{0|k}^*, k) + \mathbf{d}(\mathbf{x}_k, \mathbf{u}_{0|k}^*, k)$ and $\hat{\mathbf{x}}_{1|k} = \mathbf{f}(\mathbf{x}_k, \mathbf{u}_{0|k}^*, k)$. Substitution into the above inequality along with (2) yields:

$$\begin{aligned} \|\hat{\mathbf{x}}_{i|k+1} - \hat{\mathbf{x}}_{i+1|k}\| &\leq (\mathcal{L}_f^x)^i \|\hat{\mathbf{x}}_{0|k+1} - \hat{\mathbf{x}}_{1|k}\| \\ &\leq (\mathcal{L}_f^x)^i \|\mathbf{f}(\mathbf{x}_k, \mathbf{u}_{0|k}^*, k) + \mathbf{d}(\mathbf{x}_k, \mathbf{u}_{0|k}^*, k) \\ &\quad - \mathbf{f}(\mathbf{x}_k, \mathbf{u}_{0|k}^*, k)\| \\ &\leq (\mathcal{L}_f^x)^i \mathcal{L}_d \end{aligned}$$

Applying the Lipschitz property of b yields: $|b(\hat{\mathbf{x}}_{i|k+1}, k+i+1) - b(\hat{\mathbf{x}}_{i+1|k}, k+i+1)| \leq \mathcal{L}_b^x \mathcal{L}_d (\mathcal{L}_f^x)^i$, which implies

that, for all $i \in \{0, \dots, N-1\}$:

$$b(\hat{\mathbf{x}}_{i|k+1}, k+i+1) \geq b(\hat{\mathbf{x}}_{i+1|k}, k+i+1) - \mathcal{L}_b^x \mathcal{L}_d (\mathcal{L}_f^x)^i \quad (32)$$

Recall that if $\mathbf{x}_k \in \mathcal{C}_{pb}(k)$, for $i \in \{0, \dots, N-2\}$ $b(\hat{\mathbf{x}}_{i+1|k}, k+i+1) \geq (i+1)\Delta + \mathcal{L}_b^x \mathcal{L}_d \sum_{j=0}^i (\mathcal{L}_f^x)^j$, which yields:

$$\begin{aligned} b(\hat{\mathbf{x}}_{i|k+1}, k+i+1) &\geq b(\hat{\mathbf{x}}_{i+1|k}, k+i+1) - \mathcal{L}_b^x \mathcal{L}_d (\mathcal{L}_f^x)^i \\ &\geq (i+1)\Delta + \mathcal{L}_b^x \mathcal{L}_d \sum_{j=0}^i (\mathcal{L}_f^x)^j \\ &\quad - \mathcal{L}_b^x \mathcal{L}_d (\mathcal{L}_f^x)^i \\ &= (i+1)\Delta + \mathcal{L}_b^x \mathcal{L}_d \sum_{j=0}^{i-1} (\mathcal{L}_f^x)^j \\ &\geq i\Delta + \mathcal{L}_b^x \mathcal{L}_d \sum_{j=0}^{i-1} (\mathcal{L}_f^x)^j \end{aligned}$$

Thus $\{\xi_{l|k+1}^+\}_{l=0}^{N-2} = 0$ satisfies (20e) for the chosen $\{\mathbf{u}_{l|k+1}^+\}_{l=0}^{N-3}$ and resulting $\{\hat{\mathbf{x}}_{l|k+1}\}_{l=0}^{N-2}$.

For $\xi_{N-1|k+1}^+$, we note since $\mathcal{X}_f^N(0, k+N) \subset \mathcal{X}^N(0, k+N)$ from Assumption 10, $h(\hat{\mathbf{x}}_{N|k}, k+N) \geq \mathcal{L}_h^x \mathcal{L}_d (\mathcal{L}_f^x)^{N-1} \implies b(\hat{\mathbf{x}}_{N|k}, k+N) \geq N\Delta + \mathcal{L}_b^x \mathcal{L}_d \sum_{j=0}^{N-1} (\mathcal{L}_f^x)^j$. Substitution into (32) for $i = N-1$ yields:

$$\begin{aligned} b(\hat{\mathbf{x}}_{N-1|k+1}, k+N) &\geq b(\hat{\mathbf{x}}_{N|k}, k+N) - \mathcal{L}_b^x \mathcal{L}_d (\mathcal{L}_f^x)^{N-1} \\ &\geq N\Delta + \mathcal{L}_b^x \mathcal{L}_d \sum_{j=0}^{N-1} (\mathcal{L}_f^x)^j \\ &\quad - \mathcal{L}_b^x \mathcal{L}_d (\mathcal{L}_f^x)^{N-1} \\ &= N\Delta + \mathcal{L}_b^x \mathcal{L}_d \sum_{j=0}^{N-2} (\mathcal{L}_f^x)^j \\ &\geq (N-1)\Delta + \mathcal{L}_b^x \mathcal{L}_d \sum_{j=0}^{N-2} (\mathcal{L}_f^x)^j \end{aligned}$$

Thus $\xi_{N-1|k+1}^+ = 0$ satisfies (20e) for the chosen $\mathbf{u}_{N-2|k+1}^+$ and resulting $\hat{\mathbf{x}}_{N-1|k+1}$.

For $\xi_{N|k+1}^+$, we substitute h with associated Lipschitz constant \mathcal{L}_h^x (note the same analysis applies to h) into (32) for $i = N-1$, which yields:

$$\begin{aligned} h(\hat{\mathbf{x}}_{N-1|k+1}, k+N) &\geq h(\hat{\mathbf{x}}_{N|k}, k+N) - \mathcal{L}_h^x \mathcal{L}_d (\mathcal{L}_f^x)^{N-1} \\ &\geq \mathcal{L}_h^x \mathcal{L}_d (\mathcal{L}_f^x)^{N-1} - \mathcal{L}_h^x \mathcal{L}_d (\mathcal{L}_f^x)^{N-1} \\ &\geq 0 \end{aligned}$$

Thus $\hat{\mathbf{x}}_{N-1|k+1} \in \mathcal{C}(k+N)$ and $\bar{\mathcal{K}}(\hat{\mathbf{x}}_{N-1|k+1}, k+N) \neq \emptyset$ since h is an N -step robust, discrete-time barrier function. Thus from (30), $\mathbf{u}_{N-1|k+1}^+ \in \bar{\mathcal{K}}(\hat{\mathbf{x}}_{N-1|k+1}, k+N)$. By definition, this implies that $h(\hat{\mathbf{x}}_{N|k+1}, k+N+1) = h(\mathbf{f}(\hat{\mathbf{x}}_{N-1|k+1}, \mathbf{u}_{N-1|k+1}^+, k+N), k+N+1) \geq \mathcal{L}_h^x \mathcal{L}_d (\mathcal{L}_f^x)^{N-1}$. Thus $\xi_{N|k+1}^+ = 0$ satisfies (20f) for the chosen control $\mathbf{u}_{N-1|k+1}^+$ and resulting $\hat{\mathbf{x}}_{N|k+1}$.

We have thus constructed a feasible solution of $\{\mathbf{u}_{l|k+1}^+\}_{l=0}^{N-1}$, $\{\xi_{l|k}^+\}_{l=0}^N = 0$ for which all the constraints of $\mathcal{P}_{feas}(\mathbf{x}_{k+1}, k+1)$ are satisfied. This implies that at the next time step, there exists a control such that $h_{pb}(\mathbf{x}_{k+1}, k+1) = 0$. Thus the output of \mathcal{P}_{sf} will enforce these same conditions and so $\mathbf{x}_{k+1} \in \mathcal{C}_{pb}(k+1)$. Since $\mathbf{x}_{k_0} \in \mathcal{C}_{pb}(k_0)$, this process can be repeated by induction for all $k \geq k_0$ such that $\mathbf{x}_k \in \mathcal{C}_{pb}(k)$ for all $k \geq k_0$. From 2), since $\mathcal{C}_{pb}(k) \subset \mathcal{X}(k)$, $\mathbf{x}_k \in \mathcal{X}(k)$ for all $k \geq k_0$ which concludes the proof.

Theorem 11 ensures safety properties for all time for the closed-loop system with the predictive control law. It is important to note that there is no explicit restriction on the size of N in order to ensure safety. Adjusting N simply provides a trade-off between computational complexity and conservatism. Smaller values of N result in smaller optimization problems to be solved and smaller robustness margins, however this will yield a more conservative control law since the system state will be forced to remain close to the robust terminal safe set. On the other hand, larger values of N result in larger optimization problems, but allow for states to deviate from the robust terminal safe set so long as at time N , the system predictions can be returned to the robust terminal safe set. Also, note that as N increases the robustness margins increase, which may violate Assumption 10.

Remark 12 (Multiple constraints) *Note that in \mathcal{P}_{feas} and \mathcal{P}_{sf} , only one constraint function, b , is enforced throughout the trajectory for readability. In practice, multiple $b_i : \mathbb{R}^n \times \mathbb{N} \rightarrow \mathbb{R}$ could be implemented in \mathcal{P}_{feas} and \mathcal{P}_{sf} so long as each b_i satisfies the same requirements as b . To be clear, the following sets would be used in place of $\mathcal{X}(k)$ and $\mathcal{X}^l(\xi, k)$ for $i \in \{1, \dots, M\}$:*

$$\mathcal{X}_i(k) := \{\mathbf{x} \in \mathbb{R}^n : b_i(\mathbf{x}, k) \geq 0\} \quad (33a)$$

$$\mathcal{X}(k) = \bigcap_{i=1}^M \mathcal{X}_i(k) \quad (33b)$$

$$\mathcal{X}_j^l(\xi, k) := \{\mathbf{x} \in \mathbb{R}^n : b_i(\mathbf{x}, k) \geq -\xi + l\Delta + \mathcal{L}_b^x \mathcal{L}_d \sum_{j=0}^{l-1} (\mathcal{L}_f^x)^j\} \quad (33c)$$

$$\mathcal{X}^l(\xi, k) = \bigcap_{i=1}^M \mathcal{X}_i^l(\xi, k) \quad (33d)$$

4 Robust Differentiable Predictive Control

In this section, the learning-based differentiable predictive control (DPC) is presented and combined with the proposed predictive safety filter to provide a unified solution for ensuring safety guarantees while exploiting the probabilistic optimality of DPC. Finally, we modify the proposed control using event-triggering schemes to present two forms of controllers to reduce online computation of the proposed control.

4.1 Nominal DPC

In DPC, an explicit control policy is trained by minimizing the expected value of the following parametric optimal control problem:

$$\min_{\mathbf{W}} \mathbb{E}_{\boldsymbol{\theta} \sim \mathcal{P}_{\boldsymbol{\theta}}} \left[\sum_{k=0}^{\bar{N}-1} (\ell(\mathbf{x}_k, \mathbf{u}_k, \mathbf{r}_k) + p(\mathbf{g}_x(\mathbf{x}_k, \mathbf{p}_x))) \right. \quad (34a)$$

$$\left. + p(\mathbf{g}_u(\mathbf{u}_k, \mathbf{p}_u)) + p(\mathbf{g}_N(\mathbf{x}_{\bar{N}}, \mathbf{p}_{\bar{N}})) \right] \quad (34b)$$

$$\text{s.t. } \mathbf{x}_{k+1} = \mathbf{f}(\mathbf{x}_k, \mathbf{u}_k, k), \quad (34c)$$

$$\mathbf{u}_k = \pi_{\mathbf{W}}(\mathbf{x}_k, \boldsymbol{\theta}_k^i) \quad (34d)$$

$$\boldsymbol{\theta}_k = \{\mathbf{x}_0, \mathbf{r}_k, \mathbf{p}_x, \mathbf{p}_u, \mathbf{p}_{\bar{N}}\} \quad (34e)$$

where the loss function is composed of the parametric MPC objective $\ell : \mathbb{R}^{n_x} \times \mathbb{R}^{n_u} \times \mathbb{R}^{n_r} \rightarrow \mathbb{R}$, the parameterized state constraints $\mathbf{g}_x(\mathbf{x}_k, \mathbf{p}_x) \leq 0$, the parameterized terminal state constraints $\mathbf{g}_N(\mathbf{x}_{\bar{N}}, \mathbf{p}_{\bar{N}}) \leq 0$, the parameterized input constraints $\mathbf{g}_u(\mathbf{u}_k, \mathbf{p}_u) \leq 0$, and the penalty function for inequality constraints given as $p(\cdot) = \|\text{ReLU}(\cdot)\|_2^2$. The problem's parameters are the components in (34e) sampled from the known distribution $\mathcal{P}_{\boldsymbol{\theta}}$. In the deep learning literature, this approach is equivalent to the learning to optimize method [31].

The advantage of the parametric form of the problem (34) is that it generalizes well to a wide class of MPC objective functions, for example, trajectory tracking error between the state and reference trajectory as well as input-related costs over a finite horizon. In addition to the loss function, the parametric constraints are treated as penalties to avoid control policies that violate constraints on the system.

The DPC algorithm requires the DPC loss function terms in (34a) and (34b) to be at least once differentiable almost everywhere. Then the formulation (34) can be implemented as a differentiable program that allows us to obtain a data-driven, predictive solution by differentiating the DPC loss function backward in time through the parameterized closed-loop dynamics [32]. The closed-loop system is constructed from a given system model (34c) and neural control policy (34d) parametrized by \mathbf{W} . This allows us to obtain

direct policy gradients and update \mathbf{W} via stochastic gradient descent. For more details on the DPC policy optimization algorithm, we refer the reader to [33].

In practice, (34) is solved offline over sampled distribution $\mathcal{P}_{\boldsymbol{\theta}}$ with m number of total samples, while the trained control policy $\pi_{\mathbf{W}}(\mathbf{x}, \boldsymbol{\theta}_k)$ is implemented online without the need for online optimization. Although DPC addresses system constraints in the formulation, DPC policy optimization algorithm in its nominal form [26] does not guarantee robust constraint satisfaction.

Remark 13 *Note that the problem in (34) does not necessarily use the same constraint functions from the safety filter. In the DPC setup, $\{\mathbf{x} \in \mathbb{R}^n : \mathbf{g}_x(\mathbf{x}_k, \mathbf{p}_x) \leq 0\}$ could be set up to define the general safety constraints from $\mathcal{X}(k)$ by setting $\mathbf{g}_x(\mathbf{x}_k, \mathbf{p}_x) = -b(\mathbf{x}_k, k)$. However, in some cases it may be advantageous to focus on certain performance objectives in the DPC setup and safety only in the safety filter.*

To address disturbances, we propose an event-triggered control policy that implements the DPC control as long as the system is safe and implements the predictive control policy (22) otherwise to ensure safety. This control policy is defined in Algorithm 1.

Algorithm 1 Event-Triggered, Safe DPC Control

- 1: Given: \mathbf{x}_k, k .
 - 2: Initialize $\mathbf{x}_{0|k} = \mathbf{x}_k$.
 - 3: **for** $l \in \{0, \dots, N-1\}$ **do**
 - 4: Define $\boldsymbol{\theta}_l$.
 - 5: Compute $\mathbf{u}_{net_{l|k}} = \pi_{\mathbf{W}}(\mathbf{x}_{l|k}, \boldsymbol{\theta}_l)$.
 - 6: Compute $\mathbf{x}_{l+1|k} = \mathbf{f}(\mathbf{x}_{l|k}, \mathbf{u}_{net_{l|k}}, k+l)$.
 - 7: **end for**
 - 8: Define $\{\mathbf{u}_{net_{l|k}}\}_{l=0}^{N-1}$.
 - 9: **if** $\{\mathbf{u}_{l|k}\}_{l=0}^{N-1} = \{\mathbf{u}_{net_{l|k}}\}_{l=0}^{N-1}$ is a feasible solution to $\mathcal{P}_{\text{feas}}(\mathbf{x}_k, k)$ with $\{\xi_{l|k}\}_{l=0}^N = \mathbf{0}$ from (20), **then**
 - 10: **return** $\mathbf{u}_{net_{0|k}}$.
 - 11: **else**
 - 12: Solve $\mathcal{P}_{\text{feas}}(\mathbf{x}_k, k)$ from (20) for $\{\xi_{l|k}^*\}_{l=0}^N$.
 - 13: Solve (22), with $\mathbf{u}_{nom} = \mathbf{u}_{net_{0|k}}$ and \mathcal{P}_{sf} from (24), for $\{\mathbf{u}_{l|k}^*\}_{l=0}^{N-1}$.
 - 14: **return** $\mathbf{u}_{0|k}^*$.
 - 15: **end if**
-

Theorem 14 *Suppose the conditions of Theorem 11 hold. Given a trained DPC control law $\pi_{\mathbf{W}} : \mathbb{R}^n \times \mathbb{R}^{n_{\boldsymbol{\theta}}} \rightarrow \mathcal{U}$, suppose the system (1) is in closed-loop with the control from Algorithm 1. If $\mathbf{x}_{k_0} \in \mathcal{C}_{pb}(k_0)$ for any $k_0 \in \mathbb{N}$, then $\mathbf{x}_k \in \mathcal{C}_{pb}(k)$ and $\mathbf{x}_k \in \mathcal{X}(k) \forall k \geq k_0, k \in \mathbb{N}$.*

PROOF. First, from Theorem 11, $\mathcal{P}_{\text{feas}}$ and \mathcal{P}_{sf} are always feasible and so the control defined by Algorithm 1 is always feasible since $\pi_{\mathbf{W}}$ is defined on all of $\mathbb{R}^n \times \mathbb{R}^{n_{\boldsymbol{\theta}}}$.

Second, there are two possible cases in Algorithm 1 that can occur at each time step k . In the first case, the DPC-based control evaluated on the horizon, $\{\mathbf{u}_{net_{l|k}}\}_{l=0}^{N-1}$, along with $\{\xi_{l|k}\}_{l=0}^N = \mathbf{0}$ is a feasible solution to \mathcal{P}_{feas} . Since this horizon satisfies \mathcal{P}_{feas} with no slack variables, then $\mathbf{x}_k \in \mathcal{C}_{pb}(k)$. By construction, $\mathbf{u}_{0|k}^* = \mathbf{u}_{net_{0|k}} = \pi_W(\mathbf{x}_{l|k}, \boldsymbol{\theta}_l)$, which is the output of Algorithm 1. Thus $\mathbf{x}_{k+1} \in \mathcal{C}_{pb}(k+1)$.

In the second case, the same control is implemented as per Theorem 11 such that $\mathbf{x}_{k+1} \in \mathcal{C}_{pb}(k+1)$ follows directly.

Since the output of Algorithm 1 keeps $\mathbf{x}_{k+1} \in \mathcal{C}_{pb}(k+1)$ if $\mathbf{x}_k \in \mathcal{C}_{pb}(k)$, and $\mathbf{x}_{k_0} \in \mathcal{C}(k_0)$, then by induction, $\mathbf{x}_k \in \mathcal{C}_{pb}(k) \forall k \geq k_0$. Since $\mathcal{C}_{pb}(k) \subset \mathcal{X}(k)$, $\mathbf{x}_k \in \mathcal{X}(k) \forall k \geq k_0$ which completes the proof.

In the special case where the conditions of Theorem 3 hold, the following simpler algorithm can be implemented.

Algorithm 2 1-Step Event-Triggered, Safe DPC Control

- 1: Given: \mathbf{x}_k, k .
 - 2: Define $\boldsymbol{\theta}_k$.
 - 3: **if** $h(\mathbf{x}_k, k) > a$ **then**
 - 4: **return** $\mathbf{u}_k = \pi_W(\mathbf{x}_k, \boldsymbol{\theta}_k)$.
 - 5: **else**
 - 6: Solve $\mathcal{P}_{feas}(\mathbf{x}_k, k)$ from (23) for ξ_k^* .
 - 7: Compute (22) with $\mathbf{u}_{nom} = \pi_W(\mathbf{x}_k, \boldsymbol{\theta}_k)$ and \mathcal{P}_{sf} from (24) for \mathbf{u}_k^* .
 - 8: **return** $\mathbf{u}_k = \mathbf{u}_k^*$.
 - 9: **end if**
-

Corollary 15 *Suppose the conditions of Theorem 3 hold. Given a trained DPC control law $\pi_W : \mathbb{R}^{n_\theta} \rightarrow \mathcal{U}$, suppose the system (1) is in closed-loop with the control from Algorithm 2. Then if $\mathbf{x}_{k_0} \in \mathcal{C}(k_0)$ for any $k_0 \in \mathbb{N}$, then $\mathbf{x}_k \in \mathcal{C}(k)$, $\forall k \geq k_0, k \in \mathbb{N}$.*

PROOF. First, the control from Algorithm 2 is always feasible via part 1) of the proof of Theorem 11.

For any $k \in \mathbb{N}$, since h satisfies the conditions of Definition 1, whenever $\mathbf{x}_k \in \mathcal{A}(k)$ there exists a control such that (4) holds, which can be written as: $h(\hat{\mathbf{x}}_{1|k}, k+1) \geq \mathcal{L}_h^x \mathcal{L}_d$. In this case, $\xi_k^* = 0$ is a solution to \mathcal{P}_{feas} of (23) and so the solution of \mathcal{P}_{sf} of (24) satisfies $\mathbf{u}_k^* \in \mathcal{K}(\mathbf{x}_k, k)$ (for \mathcal{K} defined by (7)). Now, since h satisfies the conditions of Theorem 3, $\mathcal{K}(\mathbf{x}_k, k) = \mathcal{U}$ for $\mathbf{x}_k \in \mathcal{C}(k) \setminus \mathcal{A}(k)$, so that any control in the set \mathcal{U} is acceptable. Thus Algorithm 2 returns a control $\mathbf{u}_k \in \mathcal{K}(\mathbf{x}_k, k)$ for all $\mathbf{x}_k \in \mathcal{C}(k)$, $\forall k \in \mathbb{N}$. Since $\mathbf{x}_{k_0} \in \mathcal{C}(k_0)$, the proof follows from Theorem 3.

Remark 16 *It is possible to swap π_W for any control law mapping into \mathcal{U} in Algorithms 1 and 2 as well as in Theorem 14 and Corollary 15. However the advantage of using the DPC control law is that it provides a systematic way of training a neural network to consider system objectives and constraints in one framework. This is advantageous for helping to reduce the amount of events that occur in practice so that fewer online computations are needed. This is helpful for compute-limited applications, which can focus computational resources on other mission-critical tasks.*

5 Numerical Examples

In this section, the proposed controllers from Algorithm 1 and 2 are implemented on various different systems. First, a simple, single integrator example is used to demonstrate the construction of all components. Then a two-tank is used for demonstration of the proposed methodology on a nonlinear system and to compare with the original safety filter of [9]. Finally, the proposed methodology is applied from a practical perspective to a building example comprised of nonlinear, time-varying system with time-varying constraints. For all the following examples, the following parameters were held constant: $\Delta = 5 \times 10^{-8}$, $\alpha = 1 \times 10^6$. The DPC method in all presented examples was designed and trained using the Neuromancer scientific machine learning library [34]. All code was developed in Python using the Casadi optimization module to solve \mathcal{P}_{feas} and \mathcal{P}_{sf} . For each example, the DPC control π_W was a multi-layer perceptron (MLP) of 2 layers with 32 internal states each and a Gaussian Error Linear Unit (GELU) activation. The MLP was implemented with a sigmoid scale method to ensure $\pi_W \in \mathcal{U}$.

5.1 Simple Example

In this simple example, we apply Algorithm 2 to the perturbed single integrator discretized using the standard Euler method:

$$\mathbf{x}_{k+1} = \underbrace{\mathbf{x}_k + \Delta t(\mathbf{u}_k)}_{f(\mathbf{x}_k, \mathbf{u}_k, k)} + \underbrace{\Delta t w(k)}_{d(\mathbf{x}_k, \mathbf{u}_k, k)} \quad (35)$$

where $\Delta t = 0.01$ s is the sampling time and $w(k) = \bar{w} \sin(0.5k)$ is a perturbation on the system. In this example, the perturbation amplitude is $\bar{w} = 0.02$. The input constraint set is: $\mathcal{U} = \{u \in \mathbb{R} : |u| \leq 10\}$. The barrier function used here is defined as follows:

$$h(x, k) = \varepsilon - (x - x_r(k))^2 \quad (36)$$

for $x_r(k) = \bar{r} \sin(\omega t)$, $\bar{r} = 0.5$, $\omega = 0.05$ and $\varepsilon = 0.2$. The objective is to keep the system inside the time-varying tube defined by $\mathcal{C}(k) = \{x \in \mathbb{R} : h(x, k) \geq 0\}$, similar to the continuous-time version from [4].

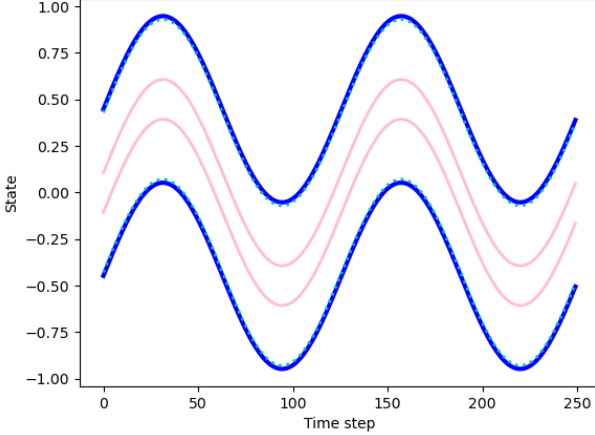


Fig. 2. (Simple example) The barrier function safe set, $\mathcal{C}(k)$, is the region between the blue, solid lines. The set $\mathcal{X}_f^N(0, k)$ is the region between the cyan, dotted lines. The set $\mathcal{A}(k)$ is the region between the pink solid lines and the blue solid lines.

In order to apply Algorithm 2, we need to ensure that h is a *robust, discrete-time barrier function* and that the conditions of Theorem 3 hold. The Lipschitz constants and bounds from Theorem 3 are computed by using standard methods for which $\mathcal{L}_h^x = 0.894$, $\mathcal{L}_h^k = 0.072$, $\mathcal{L}_d = \bar{w} = 0.02$, $\mathcal{L}_f = 0.11$, $\mathcal{L}_f^x = 1.0$. See Appendix 7.1 to check that h is a *robust, discrete-time barrier function*. Next we chose $a = \mathcal{L}_h^x(\mathcal{L}_f + \mathcal{L}_d) + \mathcal{L}_h^k = 0.180$. Since $0 < a < \varepsilon$ and $a > 0$, $\mathcal{A}(k) \neq \emptyset$ and $\mathcal{A}(k) \subset \mathcal{C}(k)$. All the conditions of Theorem 3 have been met. Figure 2 shows the sets associated with this example.

Algorithm 2 was implemented with a trained DPC control law. Since the objective is to remain inside the time-varying tube, the DPC control was used to reduce the amount of online computations needed to satisfy the objective. In order to do so, (34) was set up with $\ell(x, u, x_r) = \|x - x_r\|_2^2$ so that the DPC control attempts to stay as close to the center of the tube to avoid triggering the event in Algorithm 2. The constraint functions \mathbf{g}_x and \mathbf{g}_u along with their parameters were not used here as no state constraints were implemented for this example. For this case $\theta_k^i = x_{r_k}^i$ for which Θ is the set of reference trajectories to sample from. This set contained randomly sampled constant trajectories over the horizon $\bar{N} = 50$ with $m = 2000$ samples.

Algorithm 2 was implemented for this example along with a ‘no control’ case denoted ‘unom = 0’. This yields three different controllers. First is the ‘unom = 0’ control in which $u(x, k) = u_{nom}(x, k) = 0$ is implemented in closed-loop with the system. Second is the ‘unom = 0 + SF’ in which Algorithm 2 is implemented with $\boldsymbol{\pi}_W$ replaced with $u_{nom}(x, k) = 0$. Third is the ‘DPC + SF’ in which Algorithm 2 is implemented as stated. Figure

3 shows the results of these three scenarios.

In Figure 3, several concepts are demonstrated. First, it is clear that the ‘unom = 0’ case is not able to stay within the tube as it quickly leaves the safe set. The same control implemented in Algorithm 2, i.e., ‘unom = 0 + SF’, matches the ‘unom = 0’ control until the system attempts to leave the safe region and the safety filter acts to keep the system within the safe set. This demonstrates the basic concept that the safety filter can ensure constraint satisfaction.

Second, the results show the impact of combining the DPC control with the SF in Algorithm 2. In the ‘unom = 0 + SF’ case, the safety filter gets triggered frequently which requires the system to continually solve the non-linear program online. This is shown in Figure 3b. Note that the events only occur when the state enters $\mathcal{A}(k)$. In the ‘DPC + SF’ case, the safety filter is only solved within the first few time steps as the initial condition lies inside of $\mathcal{A}(k)$. However the DPC control is able to keep the system centered in the safe set which results in no further events triggering for the duration of the simulation. This shows that combining DPC with the safety filter allows for significant reduction in online computations, while still providing guarantees of safety in the presence of perturbations.

5.2 Two-Tank Example

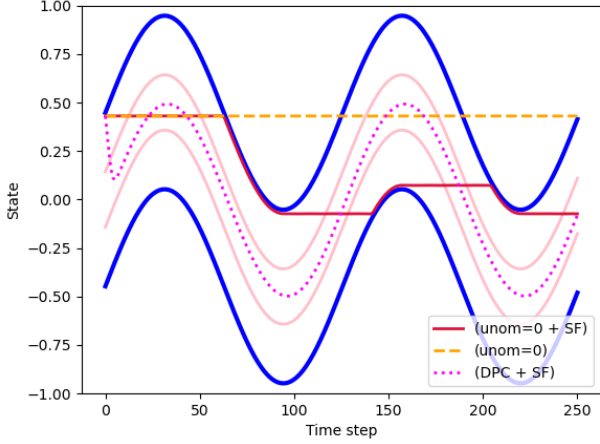
Next, we consider the nonlinear two-tank system to demonstrate robustness of the the proposed, robust methodology and to compare it with the original predictive safety filter of [9]. The two-tank system is discretized using an Euler approach shown as follows:

$$\bar{f}_1(\mathbf{x}, \mathbf{u}) := x_1 + \Delta t (c_1(1 - u_2)u_1 - c_2\sqrt{x_1}) \quad (37a)$$

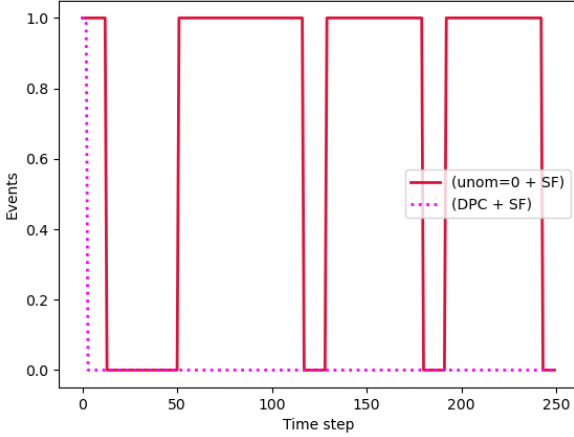
$$\bar{f}_2(\mathbf{x}, \mathbf{u}) := x_2 + \Delta t (c_1u_1u_2 + c_2\sqrt{x_1} - c_2\sqrt{x_2}) \quad (37b)$$

where $x_1, x_2 \in \mathbb{R}_{>0}$ are the height of the liquid in tank 1 and 2, respectively, $c_1 = 0.8$ is the inlet valve coefficient, $c_2 = 0.4$ is the outlet valve coefficient, and $u_1, u_2 \in \mathbb{R}_{\geq 0}$ are the pump and valve control terms, respectively. The sampling time used was $\Delta t = 0.1$ s. The objective is to keep the liquid between desired levels in each tank i.e., $\mathcal{X} = \{\mathbf{x} \in \mathbb{R}^2 : 0.2 \leq x_i \leq 1, i \in \{1, 2\}\}$ for $\mathbf{x} = [x_1, x_2]^T$, while respecting the input constraints defined by: $\mathcal{U} = \{\mathbf{u} : 0 \leq u_i \leq 1.0, \forall i \in \{1, 2\}\}$ and tracking a piece-wise constant reference trajectory $\mathbf{r} : \mathbb{N} \rightarrow \mathbb{R}^n$.

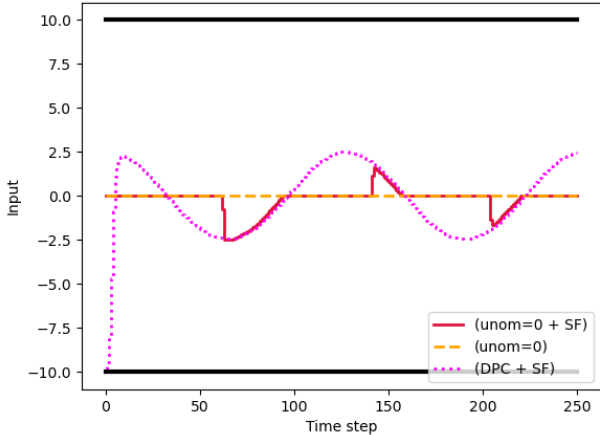
Note that some optimization solvers, such as Casadi, have difficulty when non-smooth dynamics are included in the optimization. However, thanks to the robust nature of the proposed control, we can instead re-write the two tank system with an approximation of $\sqrt{\cdot}$ and let



(a) State trajectories with barrier function safe set (blue, solid lines).



(b) Events triggered (1 is triggered, 0 is not triggered) for each simulation scenario. Note the case where $u_{nom} = 0$ is not shown as no safety filter is implemented.



(c) Input trajectories with constraint bounds (black, solid lines).

Fig. 3. (Simple example) Comparison of trajectories for ‘unom=0 + SF’ (red, solid curve), ‘unom=0’ (orange, dashed 13 curve), ‘DPC+SF’ (magenta, dotted curve).

the robust methodology handle the model mismatch:

$$f_1(\mathbf{x}, \mathbf{u}) = x_1 + \Delta t (c_1(1 - u_2)u_1 - c_2\psi(x_1)) \quad (38a)$$

$$f_2(\mathbf{x}, \mathbf{u}) = x_2 + \Delta t (c_1u_1u_2 + c_2\psi(x_1) - c_2\psi(x_2)) \quad (38b)$$

where $\psi : \mathbb{R} \rightarrow \mathbb{R}$ is a 7th order polynomial fit of \sqrt{x} on $[0.2, 1]$, which yields:

$$\begin{aligned} x_{1k+1} &= f_1(\mathbf{x}_k, \mathbf{u}_k) + (\bar{f}_1(\mathbf{x}_k, \mathbf{u}_k) - f_1(\mathbf{x}_k, \mathbf{u}_k)) + w_1(k) \\ x_{2k+1} &= \underbrace{f_2(\mathbf{x}_k, \mathbf{u}_k)}_{\mathbf{f}(\mathbf{x}_k, \mathbf{u}_k)} + \underbrace{(\bar{f}_2(\mathbf{x}_k, \mathbf{u}_k) - f_2(\mathbf{x}_k, \mathbf{u}_k))}_{\mathbf{d}(\mathbf{x}_k, \mathbf{u}_k, k)} + w_2(k) \end{aligned}$$

where $w_1(k) = w_2(k) = \bar{w}\sin(k)$ are additional perturbations acting on the system for $\bar{w} \in \mathbb{R}_{>0}$. Now we show that the conditions of Theorem 2 are satisfied. We define $h(\mathbf{x}) = \varepsilon - (x_1 - x_{r_1})^2 + \rho(x_2 - x_{r_2})^2$, $\mathbf{x}_r = [x_{r_1} = 0.63, x_{r_2} = 0.63]^T$, $b_1(\mathbf{x}) = x_{max} - x_1$, $b_2(\mathbf{x}) = x_1 - x_{min}$, $b_3(\mathbf{x}) = x_{max} - x_2$, $b_4(\mathbf{x}) = x_2 - x_{min}$, where $x_{min} = 0.2$, $x_{max} = 1.0$, $\rho = 2.69$, and b_1, b_2, b_3, b_4 are used in the proposed control as discussed in Remark 12 and note that these all have the same Lipschitz constant \mathcal{L}_b^x . The function h is shown to be an N -step robust, discrete-time barrier function in Appendix 7.2 for $N = 20$. The parameters used for the first simulation of the two-tank are as follows: $\bar{w} = 0.00001$, $\mathcal{L}_f^x = 1.205$, $\mathcal{L}_b^x = 1.0$, $\mathcal{L}_h^x = 1.331$, $\mathcal{L}_d = 0.0000542$, $\varepsilon = 0.12$, $\mathbf{x}_r = [0.63, 0.63]^T$ and $\Delta = 0.00000005$. Note that \mathcal{L}_d was determined by combining \bar{w} , the additional perturbation, with the computed bounded error between $\psi(x)$ and \sqrt{x} on $[0.2, 1.0]$.

The DPC control law for the two-tank system was designed using a regulation loss term to track the time-varying reference and penalty functions to address the system constraints. The respective terms from (34) are as follows: $\ell_{MPC}(\mathbf{x}, \mathbf{u}, \mathbf{r}) = Q_r \|\mathbf{x} - \mathbf{r}\|_2^2$, with $Q_r = 5$,

$$\mathbf{g}_x(\mathbf{x}, \mathbf{p}_x) = Q_c \begin{bmatrix} \mathbf{x} - \mathbf{x}_{max} \\ \mathbf{x}_{min} - \mathbf{x} \end{bmatrix}$$

$$\mathbf{g}_N(\mathbf{x}, \mathbf{p}_N) = Q_c \begin{bmatrix} \mathbf{x} - \mathbf{r}(N) + \varepsilon_r \\ \mathbf{r}(N) - \varepsilon_r - \mathbf{x} \end{bmatrix},$$

where \mathbf{p}_x is comprised of $\mathbf{x}_{max} = [1.0, 1.0]^T$, $\mathbf{x}_{min} = [0.2, 0.2]^T$, $\mathbf{r}(k)$, $\varepsilon_r = 0.01$, and $Q_c = 10$. For this case $\theta_k^i = \mathbf{r}_k^i$ for which Θ is the set of reference trajectories to sample from. This set contained randomly sampled constant trajectories over the horizon $\bar{N} = 50$ with $m = 2000$ samples.

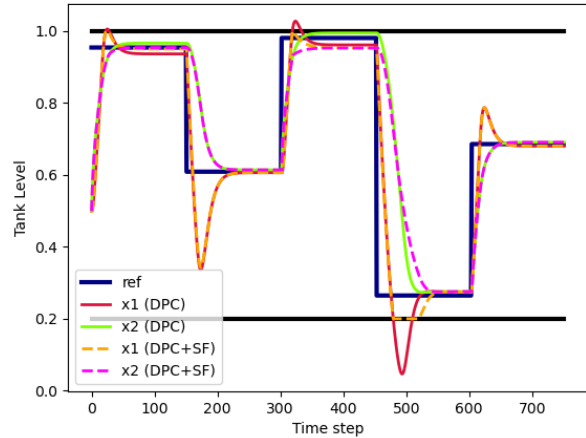
In the first set of simulations, the DPC control, denoted ‘DPC’ was implemented alone in one scenario and the proposed control (1), denoted ‘DPC+SF’, was implemented in the second scenario with $N = 20$. For the

chosen N , the conditions of Assumption 10 hold. The results of the simulation are shown in Figure 4.

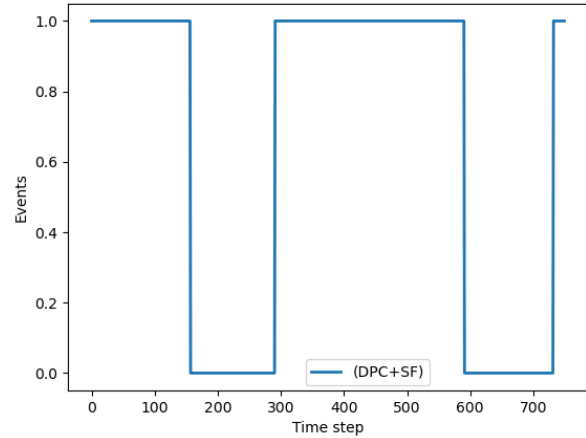
The plots in Figure 4 shows that the ‘DPC’ control is able to track the reference trajectory reasonably well, but violates the system constraints in the process. In addition to perturbation effects, this can happen in learning-based controllers when many objectives are incorporated in the loss function. The constraint violations occur at time steps $k = 24, 324$ and 493 . The ‘DPC+SF’ control on the other hand implements the ‘DPC’ control as close as possible, but then overrides the ‘DPC’ control (see Figure 4c) to ensure the states remain inside their constraint bounds (see Figure 4a). Furthermore, the event-triggering from Algorithm 1 is shown in Figure 4b for which the optimization problem from the safety filter is only solved when the system states move close to the constraint boundary. These results show the advantage of the proposed methodology from Algorithm 1 in enforcing system constraints without requiring the optimization problems to be solved at every instant when implemented online.

Although these results are promising, there is a trade-off between the size of the optimization problems from the safety filter and the magnitude of the disturbance that can be tolerated by the system. In other words, as N increases the robustness margins from (27) and (28) increase, which restricts the magnitude of \mathcal{L}_d that can be tolerated, and vice versa. To show this, we implemented the proposed control with a higher perturbation, $\bar{w} = 0.001$ for which $\mathcal{L}_d = 0.00145$, and resulted in a smaller prediction horizon of $N = 6$. The results of this simulation are shown in Figure 5. The plots show more conservative behavior in the ‘DPC+SF’ case compared to the previous simulation, especially between $k = 14$ and $k = 150$ and $k = 301$ and $k = 451$. Within both of these time intervals, the shorter prediction horizon requires the system to stay closer to \mathcal{C} to satisfy the safety conditions. Note however that the proposed control is able to reject the larger perturbation here and keep the system safe.

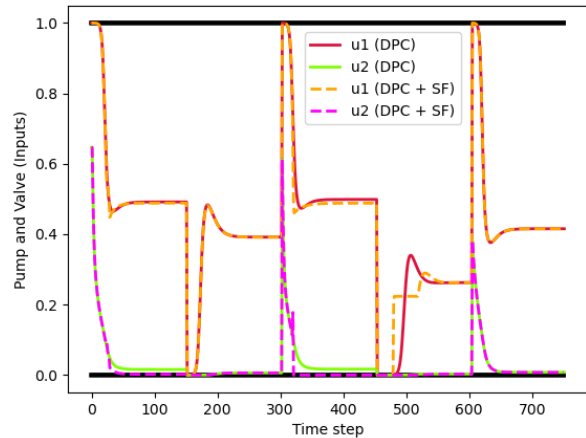
Finally, to showcase the approach compared to the existing predictive safety filter of [9], we implement the predictive safety filter on the previous example with $\bar{w} = 0.001$. Note that the two-tank is the only example in which the proposed algorithm can be compared to that of [9] because the approach from [9] is only applicable to time-invariant systems with time-invariant constraints. The same parameters used for the safety filter from Algorithm 1 were used for the safety filter of [9] for a direct comparison. The results of the safety filter implementation are shown in Figure 6, which shows similar performance to the proposed control in Figure 5, except for the state constraint violation that occurs between $k = 476$ and $k = 53$ (see Figure 6b). Furthermore, the control from [9] does not include an event-triggering and so must be solved at all instances in time. As a



(a) State trajectories with constraint bounds (black, solid lines).

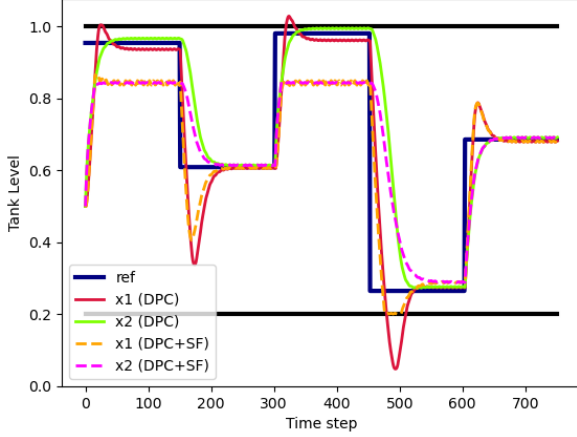


(b) Events triggered (1 is triggered, 0 is not triggered) for each simulation scenario. Note the ‘DPC’ scenario is not shown as no safety filter is implemented.

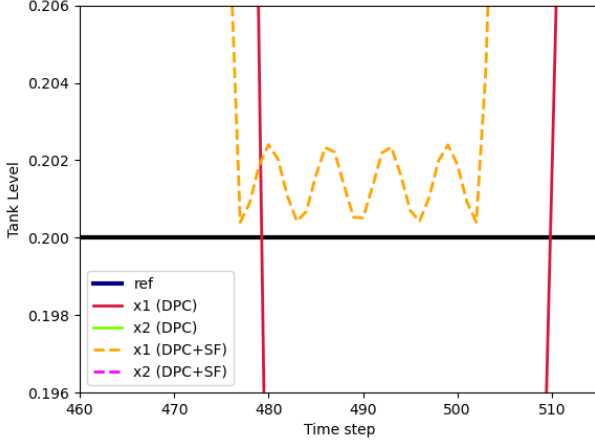


(c) Input trajectories with constraint bounds (black, solid lines).

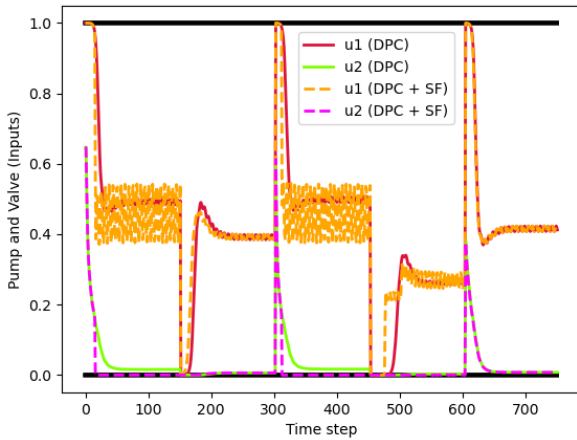
Fig. 4. (Two-tank example) Comparison of trajectories for ‘DPC’ and ‘DPC+SF’ implementations on the perturbed two-tank system with $\bar{w} = 0.00001$.



(a) State trajectories with constraint bounds (black, solid lines).



(b) State trajectories (zoomed-in) with constraint bounds (black, solid lines). Shows proposed safety filter satisfying system constraints.



(c) Input trajectories with constraint bounds (black, solid lines).

Fig. 5. (Two-tank example) Comparison of trajectories for ‘DPC’ and ‘DPC+SF’ implementations on the perturbed two-tank system with $\bar{w} = 0.001$.

result, the proposed control was 63.8% faster in online implementation compared to that of [9] (see Figure 7). These results show that the proposed control is beneficial for handling bounded perturbations to guarantee hard safety constraints at all times, while reducing the online computations required.

5.3 Building Example

Here we apply the proposed control to a simple single zone building. This is a nonlinear, time-varying system that incorporates an estimate of the ambient disturbance affecting the building, defined as follows:

$$\mathbf{x}_{k+1} = \underbrace{A\mathbf{x}_k + B\mathbf{u}_k + \hat{\mathbf{w}}(k)}_{\mathbf{f}(\mathbf{x}_k, \mathbf{u}_k, k)} + \underbrace{(\mathbf{w}(k) - \hat{\mathbf{w}}(k))}_{\mathbf{d}(k)} \quad (39)$$

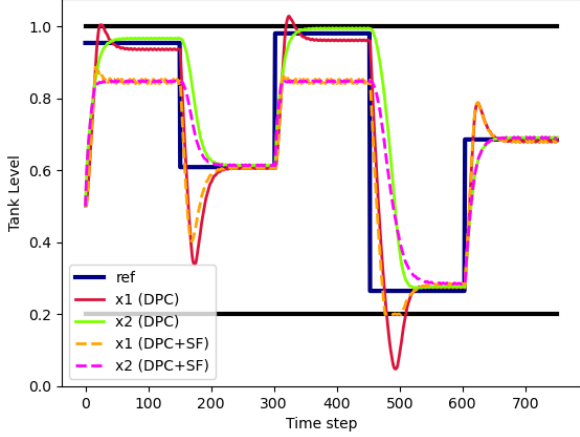
$$A = \begin{bmatrix} 0.995 & 0.0017 & 0.0 & 0.0031 \\ 0.0007 & 0.996 & 0.0003 & 0.0031 \\ 0.0 & 0.0003 & 0.983 & 0.0 \\ 0.202 & 0.488 & 0.01 & 0.257 \end{bmatrix}$$

$$B = \begin{bmatrix} 0.00000176 \\ 0.00000176 \\ 0.0 \\ 0.000506 \end{bmatrix}$$

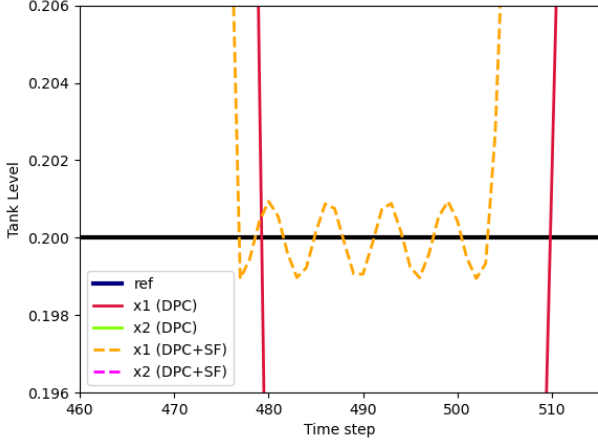
where $\mathbf{w} : \mathbb{N} \rightarrow \mathbb{R}^n$ is the perturbation of the environment affecting the system, and $\hat{\mathbf{w}} : \mathbb{N} \rightarrow \mathbb{R}^n$ is the estimate of \mathbf{w} , which is commonly approximated using annual statistical information of the building and surrounding region (see Figure 8). The model terms A and B were provided by Modelica. The control \mathbf{u} is the heat flow of the HVAC system with input constraints set: $\mathcal{U} = \{u \in \mathbb{R} : 0 \leq u \leq 5000\}$, and the number of system states is $n = 6$. Note that these dynamics were developed for a sampling rate of 0.1 s. For this example, $\mathcal{L}_d = 0.005$ and $\mathbf{d}(k) = -\mathcal{L}_d \mathbf{1}_n$ was used to demonstrate the worst-case disturbance that is constantly lowering the temperature of the building.

The objective is to minimize the control input, i.e., the output heat of the HVAC system, while remaining within time-varying comfort constraints defined by: $b_1(\mathbf{x}, k) = -C\mathbf{x} + \bar{r}(k)$, $b_2(\mathbf{x}, k) = C\mathbf{x} - r(k)$, where $C = [0, 0, 0, 1]$ maps the system state to the room temperature output and $\bar{r}, r : \mathbb{N} \rightarrow \mathbb{R}$ define the time-varying comfort constraint bounds. The two constraint functions were implemented in the proposed control as per Remark 12.

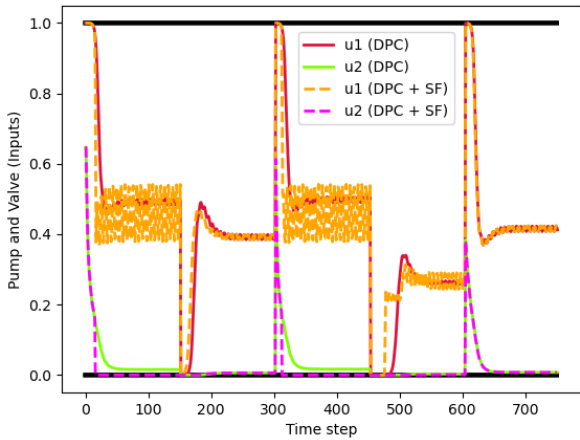
Here we take a different approach to the previous two examples and show how the proposed control could be implemented from a practical perspective. First, it is reasonable to assume that the building HVAC system is capable of keeping the building room temperature within



(a) State trajectories with constraint bounds (black, solid lines).



(b) State trajectories (zoomed-in) with constraint bounds (black, solid lines). Original safety filter violates safety constraints.



(c) Input trajectories with constraint bounds (black, solid lines).

Fig. 6. (Two-tank example) Results for predictive safety filter of [9] for ‘DPC’ and ‘DPC+SF’ implementations on the perturbed two-tank system with $\bar{w} = 0.001$.

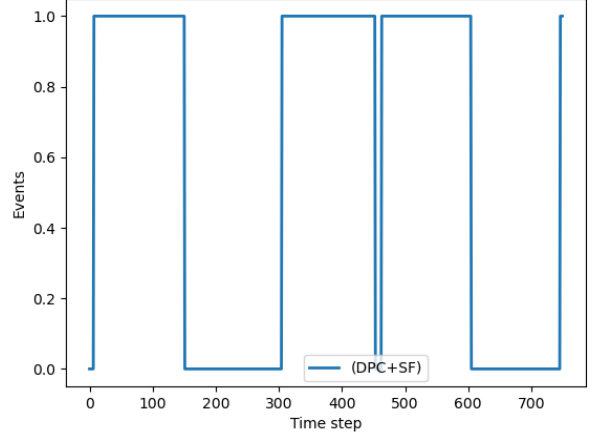


Fig. 7. (Two tank example) Events triggered (1 is triggered, 0 is not triggered) for the proposed control. Note the ‘DPC’ scenario is not shown as no safety filter is implemented.

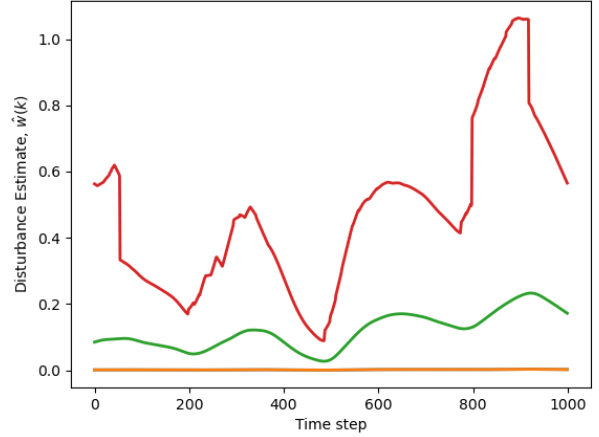


Fig. 8. Estimate of environmental perturbations on the building, $\hat{w}(k)$.

a temperature range despite, reasonable, fluctuations in the ambient temperature. Here we use a temperature range from 19.55 C to 20.45 C. We also assume, as is practical, that if the output of the system, $C\mathbf{x}$, which represents the temperature of the simple single zone, is bounded, then the states are also bounded. Thus we effectively assume the following function is a N -step robust, discrete-time barrier function:

$$h(\mathbf{x}) = \varepsilon - \|C\mathbf{x} - y_r\|_2^2 \quad (40)$$

where $\varepsilon = 0.9$, $y_r = 20$ C is the reference temperature, and $N = 6$. Note that neither the state constraint sets: $\mathcal{X}(k) = \{\mathbf{x} : b_1(\mathbf{x}, k) \geq 0, b_2(\mathbf{x}, k) \geq 0\}$, nor the terminal constraint set: $\mathcal{C} = \{\mathbf{x} : h(\mathbf{x}) \geq 0\}$ are compact, however compactness is not required for the results of

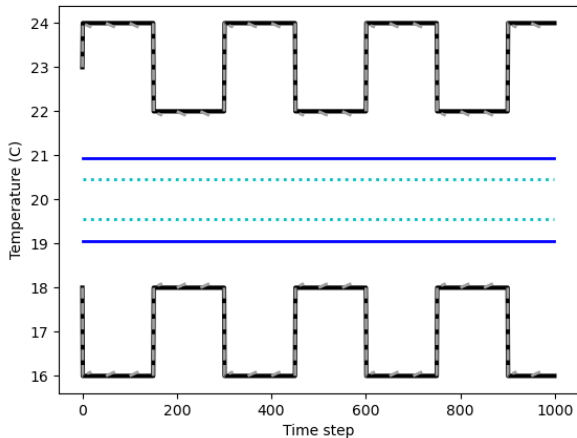


Fig. 9. (Building example) Comfort constraints (black, solid lines) along with terminal constraint (blue, solid lines). The sets from Assumption 10 are depicted as: $\mathcal{X}^l(0, k+l)$ for $l \in \{0, \dots, N\}$ is the region between the gray, dashed lines depicted at intervals of 50 time steps, $\mathcal{X}_f^N(0, k)$ is the region between the cyan, dotted lines. It is clear that $\mathcal{X}_f^N(0, k+N) \subset \mathcal{X}_k^N(0, k+N)$, $\forall k \in \mathbb{N}$ as requires by Assumption 10.

Theorem 11. We define the robustness margins used: $\mathcal{L}_f^x = 0.9998$, $\mathcal{L}_b^x = 1.0$, $\mathcal{L}_h^x = 100$. The margins for \mathcal{L}_f^x and \mathcal{L}_b^x were computed using standard methods of computing Lipschitz constants [35]. For \mathcal{L}_h^x , since h is a quadratic, we use the assumption that the states remain bounded if the temperature is bounded in the terminal set to make a conservative estimate of the bound of $\|\mathbf{x}\|$ for all $\mathbf{x} \in \mathcal{C}$.

From Figure 9, it is clear that the sets from Assumption 10 are non-empty and that the robust safety set with respect to the terminal barrier function, i.e., $\mathcal{X}_f^N(0, k+N)$, is a subset of the robust safety set with respect to the state constraints, i.e., $\mathcal{X}^N(0, k+N)$. Thus the conditions of Assumption 10 are satisfied.

The DPC control law was designed using a regulation loss term to minimize the control input of the system. In addition, a smoothness term was added to prevent sharp changes in the control input and a penalty loss was used to address state constraints. These loss terms are reflected in the following components of (34): $\ell_{\text{MPC}}(\mathbf{x}, \mathbf{u}, \mathbf{r}) = Q_u \|\mathbf{u}\|_2^2$, $\mathbf{g}_x(\mathbf{x}, \mathbf{p}_x) = Q_c [-b_1(\mathbf{x}, k), -b_2(\mathbf{x}, k)]^T$, $\mathbf{g}_u(\mathbf{u}, \mathbf{p}_u) = Q_{du}(u(k) - u(k-1))^2$ for $Q_u = 0.01$, $Q_c = 50$, and $Q_{du} = 0.1$. For this case $\theta_k^i = (\bar{r}(k)^i, \underline{r}(k)^i)$ for which Θ is the set of comfort constraint trajectories to sample from. This set contained randomly sampled constant trajectories over the horizon $\bar{N} = 100$ with $m = 1000$ samples.

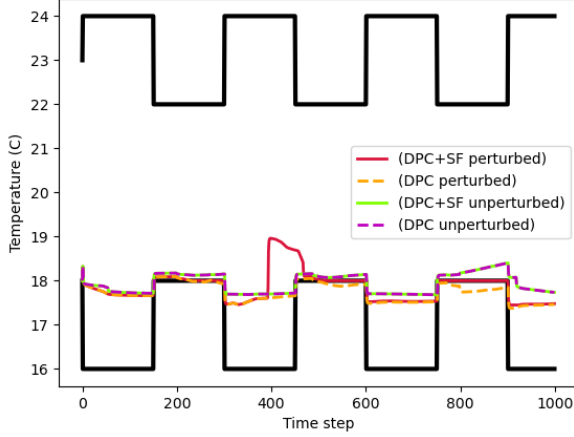
The proposed control from Algorithm 1 is compared

to using the DPC control alone. We refer to the control from Algorithm 1 as ‘DPC+SF’, and DPC run as $\mathbf{u} = \pi_W(\mathbf{x}, k)$ as simply ‘DPC’. Both controllers were run with and without the perturbation term $\mathbf{d}(k)$. The results are shown in Figure 10.

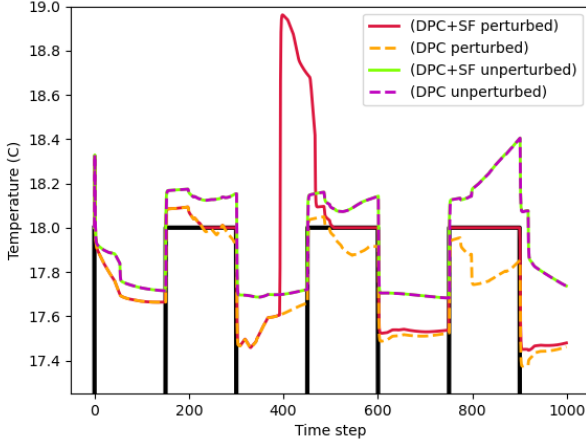
Figure 10a shows the comparisons of the various different control simulations. The unperturbed cases show that the ‘DPC+SF’ and ‘DPC’ controllers overlap throughout the entire simulation in both the temperature and input trajectories. This indicates that in the absence of uncertain disturbances, DPC is able to respect the safety constraints. If the safety constraints were ever to be violated, the safety filter would have altered the DPC control. This result is expected as DPC is known for (probabilistically) ensuring constraint satisfaction in the absence of perturbations. This is not the case with the perturbed simulations. The trajectories associated with the dynamics subject to $\mathbf{d}(k)$ show that the safety filter (see the ‘DPC+SF’ trajectories) must alter the original DPC control to remain within the comfort constraints. The ‘DPC+SF’ remains within both the comfort constraints and input constraints. The ‘DPC’ control on the other hand violates the comfort constraints (see Figure 10a). These results show that the proposed control, ‘DPC+SF’ is able to robustly handle uncertain perturbations, while remaining point-wise, minimally close to the DPC control law. Note that in this example, the objective was to reduce the amount of energy used, while staying within the comfort constraints, which resulted in trajectories close to the system constraints. As a result, the simulation resulted in events triggering at every time step. This highlights an important aspect of the event-triggering component in that if the DPC control aims to keep the system close to the constraint bounds, the safety filter will need to be solved at all time steps online.

6 Conclusion

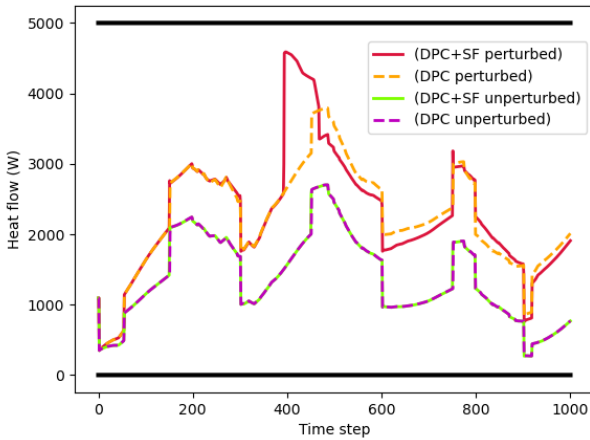
In this paper, we present a robust predictive safety filter and combine it with differentiable predictive control to provide a robust, safe, and high performance control law. The approach is applicable to time-varying systems with time-varying constraints and uses event-triggering to reduce the amount of online computation required by the method. We discuss trade-offs in the design of the proposed control and implement it on a simple single integrator, a two-tank system, and a building system to demonstrate its efficacy.



(a) Temperature trajectories with comfort constraints (black, solid lines).



(b) Temperature trajectories (zoomed-in) with comfort constraints (black, solid lines).



(c) Input trajectories with constraint bounds (black, solid lines).

Fig. 10. (Building example) Comparison of trajectories for ‘DPC+SF’ with perturbation, ‘DPC’ with perturbation, ‘DPC+SF’ without perturbation, and ‘DPC’ without perturbation. 18

7 Appendix

7.1 Barrier function check for the simple integrator

First, we define the following control to satisfy (4):

$$\hat{u}(x, k) = \begin{cases} 0, & \text{if } h(f(x, 0, k), k+1) \geq \mathcal{L}_h^x \mathcal{L}_d, \\ y(x, k) - \text{sign}(y(x, k)) \sqrt{\varepsilon - \mathcal{L}_h^x \mathcal{L}_d}, & \text{otherwise} \end{cases} \quad (41)$$

where $y(x, k) = \frac{1}{\Delta t}(-x + x_r(k+1))$. We leave it to the reader to see that (41) satisfies (4) for all $x \in \mathcal{C}(k)$, $\forall k \in \mathbb{N}$. Next we need to make sure this control satisfies the input constraints for which it can be shown that $|\hat{u}| \leq \frac{1}{\Delta t}(\mathcal{L}_h^k + \sqrt{\varepsilon} - \sqrt{\varepsilon - \mathcal{L}_h^x \bar{w}}) \leq 9.28$. Thus $\hat{u} \in \mathcal{U}$. Thus we have shown that h is a *robust, discrete-time barrier function*.

7.2 Barrier function check for the two-tank system

To show that h is a barrier function, we use a sampling-based approach, which is tractable due to the small system size of $n = 2$. To do so, we first, define a feasible control to attempt to satisfy (18). This control consists of the following components:

$$y_1(\mathbf{x}) = -\frac{1}{\Delta t}(x_1 - x_{r_1}) + c_2 \psi(x_1) \quad (42a)$$

$$y_2(\mathbf{x}) = -\frac{1}{\Delta t}(x_2 - x_{r_2}) - c_2 \psi(x_1) + c_2 \psi(x_2) \quad (42b)$$

We can now define the proposed control noting that the condition (18) is only required when $\mathbf{x}_k \in \mathcal{C}$. The condition (18) can be written as: $h(\mathbf{f}(\mathbf{x}, \mathbf{u})) = \varepsilon - \Delta t^2(c_1(1-u_2)u_1 - y_1(\mathbf{x}))^2 - \rho \Delta t^2(c_1 u_1 u_2 - y_2(\mathbf{x}))^2 \geq \mathcal{L}_h^x \mathcal{L}_d (\mathcal{L}_f^x)^{N-1}$. Thus we can define an optimal point-wise control to satisfy the condition by:

$$\hat{\mathbf{u}}(\mathbf{x}) = \min_{\mathbf{u} \in \mathcal{U}} (c_1(1-u_2)u_2 - y_1(\mathbf{x}))^2 + \rho (c_1 u_1 u_2 - y_2(\mathbf{x}))^2 \quad (43)$$

The chosen control law to show that h is a barrier function is:

$$\bar{\mathbf{u}}(\mathbf{x}) = \begin{cases} 0, & \text{if } h(\mathbf{f}(\mathbf{x}_k, 0)) \geq \mathcal{L}_h^x \mathcal{L}_d (\mathcal{L}_f^x)^{N-1}, \\ \hat{\mathbf{u}}(\mathbf{x}), & \text{otherwise} \end{cases} \quad (44)$$

The control $\bar{\mathbf{u}}$ was checked over a grid of 10,000 sampled states, equally spaced, containing \mathcal{C} defined with endpoints $\{ [0.284, 0.284]^T, [0.284, 0.976]^T, [0.976, 0.284]^T, [0.976, 0.976]^T \}$. For the two scenarios presented in Section 5.2, the sampling approach ensured that (18) held over the grid search, which suggested that h was an *N-step robust, discrete-time barrier function*.

References

- [1] A. Ames, X. Xu, J. Grizzle, and P. Tabuada, "Control barrier function based quadratic programs for safety critical systems," *IEEE Transactions on Automatic Control*, vol. 62, no. 8, pp. 3861–3876, 2017.
- [2] V. Freire and M. M. Nicotra, "Systematic Design of Discrete-Time Control Barrier Functions Using Maximal Output Admissible Sets," *IEEE Control Systems Letters*, vol. 7, pp. 1891–1896, 2023.
- [3] P. Akella and A. D. Ames, "A Barrier-Based Scenario Approach to Verifying Safety-Critical Systems," *IEEE Robotics and Automation Letters*, vol. 7, no. 4, pp. 11 062–11 069, 2022.
- [4] W. Shaw Cortez and D. V. Dimarogonas, "Safe-by-design control for Euler–Lagrange systems," *Automatica*, vol. 146, p. 110620, 2022.
- [5] A. Clark, "Verification and Synthesis of Control Barrier Functions," in *2021 60th IEEE Conference on Decision and Control (CDC)*, Dec. 2021, pp. 6105–6112.
- [6] A. Robey, H. Hu, L. Lindemann, H. Zhang, D. V. Dimarogonas, S. Tu, and N. Matni, "Learning Control Barrier Functions from Expert Demonstrations," in *2020 59th IEEE Conference on Decision and Control (CDC)*, 2020, pp. 3717–3724.
- [7] K. Long, C. Qian, J. Cortés, and N. Atanasov, "Learning barrier functions with memory for robust safe navigation," *IEEE Robotics and Automation Letters*, vol. 6, no. 3, pp. 4931–4938, 2021.
- [8] A. Wiltz, X. Tan, and D. V. Dimarogonas, "Construction of Control Barrier Functions Using Predictions with Finite Horizon," 2023.
- [9] K. P. Wabersich and M. N. Zeilinger, "Predictive control barrier functions: Enhanced safety mechanisms for learning-based control," *arXiv:2105.10241 [cs, eess]*, 2022.
- [10] J. Zeng, Z. Li, and K. Sreenath, "Enhancing Feasibility and Safety of Nonlinear Model Predictive Control with Discrete-Time Control Barrier Functions," in *2021 60th IEEE Conference on Decision and Control (CDC)*, 2021, pp. 6137–6144.
- [11] P. Roque, W. Shaw Cortez, L. Lindemann, and D. V. Dimarogonas, "Corridor MPC: Towards Optimal and Safe Trajectory Tracking," in *2022 American Control Conference (ACC)*, 2022, pp. 2025–2032.
- [12] L. Brunke, S. Zhou, and A. P. Schoellig, "Robust Predictive Output-Feedback Safety Filter for Uncertain Nonlinear Control Systems," in *2022 IEEE 61st Conference on Decision and Control (CDC)*, 2022, pp. 3051–3058.
- [13] J. Drgoña, J. Arroyo, I. Cupeiro Figueroa, D. Blum, K. Arendt, D. Kim, E. P. Ollé, J. Oravec, M. Wetter, D. L. Vrabie, and L. Helsen, "All you need to know about model predictive control for buildings," *Annual Reviews in Control*, vol. 50, pp. 190–232, 2020.
- [14] K. P. Wabersich, A. J. Taylor, J. J. Choi, K. Sreenath, C. J. Tomlin, A. D. Ames, and M. N. Zeilinger, "Data-driven safety filters: Hamilton-jacobi reachability, control barrier functions, and predictive methods for uncertain systems," *IEEE Control Systems Magazine*, vol. 43, no. 5, pp. 137–177, 2023.
- [15] T. X. Nghiem, J. Drgoña, C. Jones, Z. Nagy, R. Schwan, B. Dey, A. Chakrabarty, S. Di Cairano, J. A. Paulson, A. Carron, M. N. Zeilinger, W. Shaw Cortez, and D. L. Vrabie, "Physics-informed machine learning for modeling and control of dynamical systems," in *2023 American Control Conference (ACC)*, 2023, pp. 3735–3750.
- [16] A. Agrawal and K. Sreenath, "Discrete Control Barrier Functions for Safety-Critical Control of Discrete Systems with Application to Bipedal Robot Navigation," in *Proceedings of Robotics: Science and Systems*, 2017, pp. 1–10.
- [17] Y. Xiong, D.-H. Zhai, M. Tavakoli, and Y. Xia, "Discrete-Time Control Barrier Function: High-Order Case and Adaptive Case," *IEEE Transactions on Cybernetics*, pp. 1–9, 2022.
- [18] R. Takano, H. Oyama, and M. Yamakita, "Application of Robust Control Barrier Function with Stochastic Disturbance Model for Discrete Time Systems," *IFAC-PapersOnLine*, vol. 51, no. 31, pp. 46–51, 2018.
- [19] R. K. Cosner, P. Culbertson, A. J. Taylor, and A. D. Ames, "Robust Safety under Stochastic Uncertainty with Discrete-Time Control Barrier Functions," 2023.
- [20] M. Ahmadi, A. Singletary, J. W. Burdick, and A. D. Ames, "Safe Policy Synthesis in Multi-Agent POMDPs via Discrete-Time Barrier Functions," in *2019 IEEE 58th Conference on Decision and Control (CDC)*, 2019, pp. 4797–4803.
- [21] J. Zeng, B. Zhang, and K. Sreenath, "Safety-Critical Model Predictive Control with Discrete-Time Control Barrier Function," in *2021 American Control Conference (Acc)*. New York: Ieee, 2021, pp. 3882–3889.
- [22] S. Liu, J. Zeng, K. Sreenath, and C. A. Belta, "Iterative Convex Optimization for Model Predictive Control with Discrete-Time High-Order Control Barrier Functions," 2022.
- [23] A. Thirugnanam, J. Zeng, and K. Sreenath, "Safety-Critical Control and Planning for Obstacle Avoidance between Polytopes with Control Barrier Functions," in *2022 International Conference on Robotics and Automation (ICRA)*, 2022, pp. 286–292.
- [24] M. H. Cohen, C. Belta, and R. Tron, "Robust Control Barrier Functions for Nonlinear Control Systems with Uncertainty: A Duality-based Approach," in *2022 IEEE 61st Conference on Decision and Control (CDC)*, 2022, pp. 174–179.
- [25] X. Tan and D. V. Dimarogonas, "Compatibility checking of multiple control barrier functions for input constrained systems," in *2022 IEEE 61st Conference on Decision and Control (CDC)*, 2022, pp. 939–944.
- [26] J. Drgoña, K. Kiš, A. Tuor, D. Vrabie, and M. Klaučo, "Differentiable predictive control: Deep learning alternative to explicit model predictive control for unknown nonlinear systems," *Journal of Process Control*, vol. 116, pp. 80–92, Aug. 2022.
- [27] W. Shaw Cortez, J. Drgoña, A. Tuor, M. Halappanavar, and D. Vrabie, "Differentiable predictive control with safety guarantees: A control barrier function approach," in *2022 IEEE 61st Conference on Decision and Control (CDC)*, 2022, pp. 932–938.
- [28] S. Mukherjee, J. Drgoña, A. Tuor, M. Halappanavar, and D. Vrabie, "Neural lyapunov differentiable predictive control," in *2022 IEEE 61st Conference on Decision and Control (CDC)*, Dec. 2022, pp. 2097–2104.
- [29] F. Blanchini and S. Miani, *Set-Theoretic Methods in Control*, ser. Systems & Control : Foundations & Applications. Birkhäuser, 2015.
- [30] J. Rawings, D. Mayne, and M. M. Diehl, *Model Predictive Control: Theory, Computation, and Design*, 2nd ed. Santa Barbara, CA, USA: Nob Hill Publishing, 2017.
- [31] P. L. Donti, D. Rolnick, and J. Z. Kolter, "DC3: A learning method for optimization with hard constraints," in *International Conference on Learning Representations*, 2021. [Online]. Available: <https://openreview.net/forum?id=V1ZHvxJ6dSS>

- [32] G. Puskorius and L. Feldkamp, "Truncated backpropagation through time and Kalman filter training for neurocontrol," in *Proceedings of 1994 IEEE International Conference on Neural Networks (ICNN'94)*, vol. 4. IEEE, 1994, pp. 2488–2493.
- [33] J. Drgona, A. Tuor, and D. Vrabie, "Learning constrained adaptive differentiable predictive control policies with guarantees," *arXiv preprint arXiv:2004.11184*, 2022.
- [34] J. Drgona, A. Tuor, J. Koch, M. Shapiro, and D. Vrabie, "NeuroMANCER: Neural Modules with Adaptive Nonlinear Constraints and Efficient Regularizations," 2023. [Online]. Available: <https://github.com/pnml/neuromancer>
- [35] H. K. Khalil, *Nonlinear Systems*. Upper Saddle River, N.J. : Prentice Hall, c2002., 2002.